Pathological studies on hantavirus using hemorrhagic fever with renal syndrome mouse model and development of a novel serodiagnosis method for shrew-borne hantaviruses

（腎症候性出血熱マウスモデルを用いたハンタウイルスの病原性解析及び新規トガリネズミ由来ハンタウイルスの血清診断法開発）

危 卓行

Wei Zhuoxing

Contents

Figures and Tables

Abbreviations

ASAV Asama virus

ALT alanine transaminase

ALTV Altai virus

BUN blood urea nitrogen

cDNA complementary deoxyribonucleic acid

CKDu chronic kidney disease of unknown etiology

DMEM Dulbecco’s modified eagle medium

DNA deoxyribonucleic acid

dpi day post inoculation

FBS fetal bovine serum

FFU focus forming units

GP glycoprotein

HPS hantavirus pulmonary syndrome

HE hematoxylin and eosin

HFRS hemorrhagic fever with renal syndrome

HTNV Hantaan orthohantavirus

IHC immunohistochemistry

IgG immunoglobulin G

KHF Korean hemorrhage fever

KIM kidney injury molecule

L large

M medium

mAb monoclonal antibody

MEM minimum essential medium

mg milligram

ml milliliter

µg microgram

µl microliter

N nucleocapsid

NC negative control

NE nephropathia epidemica

ORF open reading frame

PBS phosphate buffered saline

PCR polymerase chain reaction

PUUV Puumala orthohantavirus

RT-PCR real-time polymerase chain reaction

rGP recombinant glycoprotein

rN recombinant nucleocapsid

RNA ribonucleic acid

SEOV Seoul orthohantavirus

SWSV Seewis virus

THAIV Thailand orthohantavirus

TPMV Thottapalayam thottimvirus

TNF- α tumor necrosis factor α

VSV vesicular stomatitis virus

WBC white blood cell

Notes

This thesis contains two chapters, and they have been published as follows:

1. Wei Z, Shimizu K, Nishigami K, Tsuda Y, Sarathukumara Y, Muthusinghe DS, Gamage CD, Granathne L, Lokupathirage SMW, Nanayakkara N, Arikawa J, Kikuchi F, Tanaka-Taya K, Suzuki M, Morikawa S, Arai S, Yoshimatsu K. Serological methods for detection of infection with shrew-borne hantaviruses: Thottapalayam, Seewis, Altai, and Asama viruses. Arch Virol, 166: 275-280, 2021

2. Wei Z, Shimizu K, Sarii RS, Muthusinghe DS, Lokupathirage SMW, Nio-Kobayash J, Yoshimatsu K. Pathological studies on Hantaan virus-infected mice simulating severe hemorrhagic fever with renal syndrome. Viruses, 14(10):2247, 2022

Preface

The viruses in the family *Hantaviradae* comprise negative-sense RNA viruses belonging to the order Bunyavirales. In the subfamily Mammantavirinae, four genera and 47 viruses have been registered with the International Committee on Taxonomy of Viruses and new viruses are continuously being identified. The viruses related to this study are listed in Table 1. Viruses in the subfamily Mammantavirinae, genus *Orthohantavirus*, cause asymptomatic chronic infection in their natural hosts, and transmission occurs *via* the inhalation of host excreta or biting due to the presence of viruses in saliva[42]. Humans are considered a dead-end host. Infections of humans with rodent-borne orthohantaviruses result in two clinical outcomes hemorrhagic fever with renal syndromes (HFRS) in Europe and Asia, and hantavirus pulmonary syndrome (HPS) in the Americas[20, 17]. HFRS encompasses several diseases, Korean hemorrhagic fever (KHF), nephropathia epidemica (NE), and epidemic hemorrhagic fever. Although it is becoming increasingly clear that the clinical differences between HFRS and HPS are less distinct, with more frequent detection of respiratory disease in patients with HFRS and kidney involvement in patients with HPS, the mechanisms that determine whether hantaviruses mainly exhibit virulence in the lungs or the kidneys are still unclear. Jangra *et al.* reported that the causative viruses of HPS use the lung protocadherin-1 molecule for cell entry, which may explain the lung tropism of viruses causing HPS[31]. On the other hand, the molecules that determine the viruses causing HFRS have not yet been identified.

In many countries, HFRS and HPS have already become a significant public health problem. In China, approximately 10,000–20,000 cases of HFRS are reported annually, while Korea and Russia report 300–900 cases each year[38]. Several pathogenic hantavirus strains circulate in the Samara and Bashkirtosatan regions, which is the most HFRS-endemic region in western Russia[1]. In contrast, in Europe where NE is highly endemic, 100–300 cases are reported annually in Sweden, as well as 1000 cases in Finland[55]. In Germany, 1688 and 2017 cases were reported in 2007 and 2010, respectively[18,19,28]. HPS cases have been reported in 29 states of the USA and three provinces of Canada, while outbreaks and sporadic cases have also been reported in Argentina, Brazil, Chile, Paraguay, Bolivia, and Uruguay[90]. The geographical distribution of rodent hosts generally determines the area in which hantavirus disease occurs. More than 70% of HFRS cases occur in rural regions with poor housing conditions and high rodent populations, and most patients are local farmers, who live or work near infected rodents and are therefore at a high risk of infection[91, 33].

HFRS mortality varies with causative virus species, and ranges from 0.1–0.2% for *Puumala orthohantavirus* (PUUV), to 10–15% for *Hantaan orthohantavirus* (HTNV) and *Dobrava orthohantavirus* (DOBV) infections. Infection with new world hantaviruses responsible for HPS in the Americas are associated with a higher fatality rate, averaging 45% without specific treatment[90]. The pathogenicity of shrew and bat-borne hantaviruses in humans is still unknown.

Since hantaviruses are widely distributed worldwide and hundreds of thousands HFRS cases are reported, particularly in Asian countries, it is important to understand

HFRS pathogenesis. HFRS is clinically characterized by fever, headache, abdominal discomfort, acute kidney injury, and hemorrhage[37]. HFRS can present as mild, moderate, or severe illness, depending on the causative virus; PUUV can cause mild HFRS, while Seoul virus causes moderate illness, and DOBV and HTNV cause severe HFRS[33]. The cause of these differences in HFRS severity is still unknown.

Although the direct effects of immune response to hantavirus-infected cells are not thought to contribute to pathogenesis, HFRS pathogenesis is still not fully understood. A suitable animal model for HFRS has not yet been established. In experimental infections, immunocompromised animals showed different clinical outcomes from human cases and immunocompetent animals were infected asymptomatically. This study focused on the report that laboratory mice infected with HTNV strain Korean hemorrhage fever virus (KHFV) exhibited renal hemorrhage similar to that in severe HFRS. KHFV was closed to prototype HTNV strain 76-118 in phylogenetic analysis (Fig. 1), but the virulence in mice was significantly different from that of prototype infection. Furthermore, a single amino acid mutation on KHFV glycoprotein reduced the virulence. This model was useful for investigating HFRS pathogenesis[71]. However, pathological studies for HFRS model mice, such as cell-tropism, proliferation in organs, histopathological analysis, and clinicopathological analysis, were not fully performed in the present study. Therefore, the comparison of this mouse model and human HFRS cases is needed to confirm pathological similarity.

Since *Thottopalayam thottimvirus* (TPMV) was first isolated from Asian house shrews (*Suncus murinus*) captured in India in 1964[13], various shrew-borne hantaviruses

have been reported worldwide[82]. Although the infectivity and pathogenicity of these viruses to humans are still unknown, it is important to confirm if these viruses are related to some HFRS or HPS-like diseases or are of uncertain etiology. For example, chronic kidney disease of unknown etiology (CKDu) places a substantial burden on public health in Sri Lankan agricultural communities[10, 65]. Since high seroprevalences of hantavirus infection have been reported in patients with CKDu in several locations in Sri Lanka, Thailand-like orthohantavirus infection might be a potential risk factor for CKDu[68]. More evidence is needed to prove if hantavirus pathogenicity is involved in the development of CKDu.

In this study, pathological experiments were conducted on an HFRS mouse model to elucidate the pathogenicity of hantavirus-associated HFRS. Furthermore, a serological diagnostic method was established for shrew-borne hantavirus infection and the relationship between the prevalence of these viruses and CKDu in Sri Lanka was investigated.

Table 1 Viruses belonging to family *hantaviridae*, subfamily *mammantavirinae*

Genus	Viruses	Host animal	Disease	Distribution of virus	Reference
Orthohantavirus	Hantaan (HTNV)	*Apodemus agraius*	Severe HFRS KHF	Asia, Europe	Lee et a.l, 1978[46]
Orthohantavirus	Seoul (SEOV)	*Rattus rattus, R. norvegicus*	Moderate HFRS	World-wide	Lee et al., 1982[44]
Orthohantavirus	Dobrava (DOBV)	*Apodemus flavicollis*	Severe HFRS	Balkans, Russia, Estonia	Avsic-Zupanc et al., 1994[11]
Orthohantavirus	Thailand (THAIV)	*Bandicota indica*	Unknown	Thailand	Pattamadilok et al., 2006[62]
Orthohantavirus	Puumala (PUUV)	*Clethrionomys glarelus*	Mild HFRS/NE	Europe, Balkans, Russia	Brummer et al., 1980[12]
Orthohantavirus	Andes (ANDV)	*Oligoryzomys longicaudatus*	HPS	Argentina	Gorbunova et al., 2010[24]
Orthohantavirus	Asama (ASAV)	*Urotruchus talpoides*	Unknown	Japan	Arai S et al., 2008[3]
Orthohantavirus	Seewis (SWSV)	*Sorex araneus*	Unknown	Europe, Russia	Ling J et al., 2014[48]
Thottimovirus	Thottapalayam (TPMV)	*Suncus Murinus*	Unknown	India	Carey DE et al., 1971[13]
Unclasified	Altai (ALTV)	*Sorex caecutiens*	Unknown	Russia, Europe, Mongolia	Kang HJ et al., 2019[34]

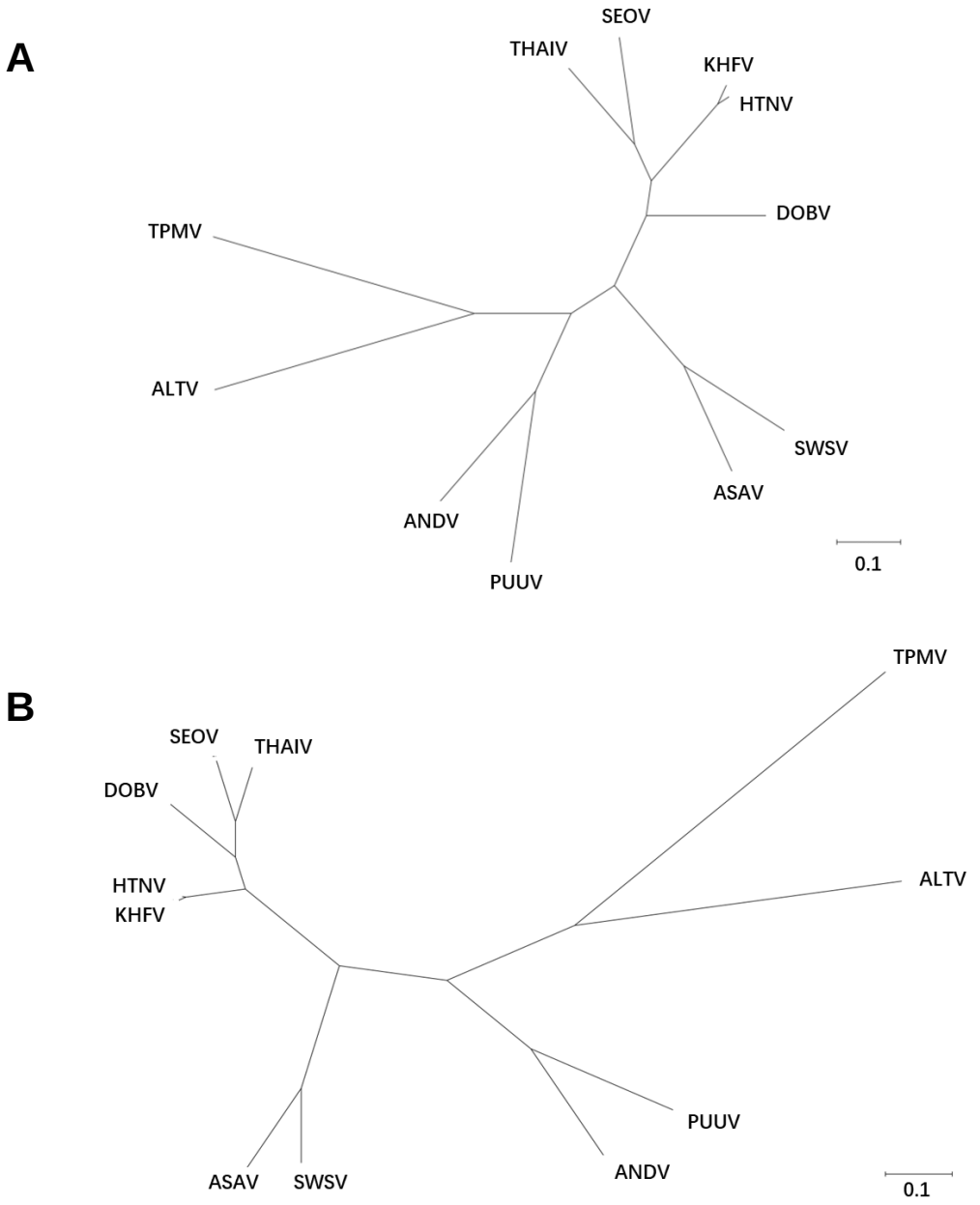

Figure 1 Phylogenetic tree of hantaviruses based on (A) M-segment ORF sequences and (B) deduced amino acid sequences.

The hantavirus M-segment sequences were analyzed by Neighbor joining method in PHYLIP run on GENETYX-Mac version 21 (Genetyx, Tokyo, Japan). The scale bar indicates a sequence divergence of 0.1. The sequences accession numbers were listed below: HTNV (KT885048.1), SEOV (OK500097.1), DOBV (OM677635.1), THAIV (MZ343361.1), PUUV (OM372470.1), ANDV (MN095822.1), ASAV (NC_038274.1), SWSV (KY651022.1), TPMV (NC_010708.1), ALTV (MK340903.1), and two KHFV sequences, KHF4 (LC209208) and KHF5 (LC209209).

Chapter 1: Pathological studies on Hantaan virus-infected mice simulating severe hemorrhagic fever with renal syndrome

1. Introduction

Orthohantaviruses are enveloped single-stranded negative-sense RNA viruses that belong to the family *Hantaviridae* and the order *Bunyavirales* [30]. Orthohantaviruses are responsible for two fatal rodent-borne zoonotic diseases in humans: HFRS [47] and HPS [57]. HFRS is caused by Old World hantaviruses, such as the HTNV [47], SEOV [45], DOBV[11], and PUUV[12]. Among the above viruses, millions of HTNV infections have been reported over the past 50 years and it is considered one of the most important viruses in East Asia, and its specific anti-viral agents have not yet been established. Inactivated hantavirus vaccines were developed in China and Korea and clinical trials of DNA vaccines are underway in the United States[29,34,51]. However, most countries do not have a licensed vaccine.

The mechanism underlying HFRS pathogenesis has not yet been elucidated. VE-cadherin cell-signaling is one of the candidates associated with vascular hyperpermeability[24], and reportedly, bradykinin plays a major role in microvascular hyperpermeability[76,78]. The use of the bradykinin antagonist led to the successful treatment of a patient with severe HFRS caused by the Puumala virus infection in Europe, supporting the report by Taylor et al[77]. Inflammatory cytokines are also considered to be associated with pathogenesis of hantavirus[22,36,40]. Interleukin -6 (IL-6) and other inflammatory cytokines are the key to cytokine release syndrome/cytokine storm, causing further inflammatory cytokine outburst[44].

Animal models are important for analyzing viral pathogenicity and planning anti-viral strategies. Among them, the laboratory mice are useful experimental animals as a lot of background information and research tools are available. However, laboratory mice rarely exhibit symptoms after inoculation with hantaviruses. Neonatal and severely immunodeficient mice often show symptoms such as encephalitis,

pneumonia, and wasting syndrome, which are not typical HFRS symptoms[39,75,87]. Recently, *Nlrc3* knockout mice infected with HTNV exhibited innate immune disorders, with symptoms similar to HFRS[53]. Therefore, HFRS models using immunocompetent mice are required for the evaluation of anti-viral agents and vaccines.

Previously, it has reported that the HTNV strain Korean hemorrhagic fever virus (KHFV) causes weight loss and renal medullary hemorrhage in mice and can be used as a model for HFRS[71]. CD8+ T cells are involved in renal hemorrhage in this model[72]. The report has shown that a single amino acid substitution E417K is present in the envelope glycoprotein (GP) in the avirulent clone-4 (KHF4) compared to KHFV[71]. Although this amino acid exchange was not localized within T-cell epitope, a T-cell response was observed, even with KHF4 infection. Thus, the difference in response between the virulent clone-5 (KHF5) and avirulent strain KHF4 in mice has not been understood yet.

In this study, I clarified the viral tissue tropism in mice infected with KHF4 and KHF5. By clarifying the mechanism of HFRS-like symptoms, I sought to demonstrate their suitability as an HFRS model by the comparison of biological markers. Further, I have evaluated the role of the E417K mutation in envelope GP.

2. Materials and methods

2.1 Viruses and cells

The HTNV strain KHFV was isolated from the blood of a patient with Korean hemorrhagic fever and passaged 10 times in the brains of newborn jcl:ICR mice[9]. Five clones of KHFV were obtained by plaque purification in Vero E6 cells (ATCC CRL1586) [9,71]. Among them, two clones, KHF4 and KHF5, were used in this study. The HTNV strain 76–118 derived from *Apodemus agrarius* was used as a prototype reference[47]. The HTNV strains were propagated in Vero E6 cells maintained in Eagle's Minimum Essential Medium (MEM) (Gibco; Thermo Fisher Scientific, Carlsbad, CA, USA) supplemented with 5% heat-inactivated fetal bovine serum (FBS; Biowest, Nuaillé, France), 1% MEM non-essential amino acids (Gibco; Thermo Fisher Scientific), 1% insulin-transferrin-selenium (Fujifilm Wako, Osaka, Japan), 1% penicillin (50 units/ml), streptomycin (50 μg/ml; Nacalai Tesque, Kyoto, Japan), and 1% gentamicin (100 μg/ml; Nacalai Tesque). Virus infectivity titers were determined as described previously[9].

U937 cells (JCRB cell bank #9021) were purchased from the JCRB Cell Bank and maintained in RPMI 1640 medium (Thermo Fisher Scientific) with 10% FBS (Biowest, Nuaillé, France) and 1% penicillin-streptomycin (Nacalai Tesque). The human adenocarcinoma cell line A549, human embryonic kidney cells, and HEK293T cells (Riken, Japan) were maintained in Dulbecco's Modified Eagle Medium (DMEM) (Thermo Fisher Scientific) with 10% FBS and 1% penicillin-streptomycin.

Splenocytes from mice were prepared as described previously[5]. Splenocytes were maintained in RPMI 1640 medium with 10% FBS, 50 μM 2-mercaptoethanol (Fujifilm Wako), 1% penicillin-streptomycin, and 1% gentamicin (Nacalai Tesque).

Dendritic cells were separated from splenocytes using the CD11c Microbeads ultrapure kit (Miltenyi Biotec, Bergisch Gladbach, Germany) as per the manufacturer's protocols. Peritoneal cells were collected, and adherent cells were used as the peritoneal macrophage fraction.

2.2 Indirect immunofluorescence assay (IFA)

Vero E6 cells were fixed with acetone one-day post inoculation (dpi) with KHF4 and KHF5. Vero E6 cells expressing the recombinant envelope glycoproteins (rGP) for KHF4 and KHF5 were fixed with acetone two days after transfection (described below). Hybridoma culture supernatants with the dilutions 1:1, 1:10, and 1:100, and secreting monoclonal antibodies targeting HTNV GPs[7] were used. Alexa Fluor 488-conjugated goat anti-mouse immunoglobulin G (IgG) (Invitrogen, Thermo Fisher Scientific, A-11029) was used as a secondary antibody at 1:1000 dilution.

2.3 Cell fusion assay

The cell fusion assay was performed as described previously with a few modifications[8]. The KHFV-inoculated and rGP-expressing Vero E6 cells (see next section) were treated with prewarmed (37 °C) acetate buffered saline adjusted to pH 5.8 for 2 min. The medium was subsequently replaced with growth medium and incubated at 37 °C for 16 h. The cells were washed with PBS, fixed with 10% formalin in PBS, and stained with Giemsa (Merck, Darmstadt, Germany).

2.4. Comparison of KHF4 and KHF5 growth in Vero E6 cells

Viruses were inoculated into Vero E6 cell monolayers in 6-well plates at a multiplicity of infection (MOI) = 0.1, and the medium was replaced with fresh medium

after 1 h of incubation. Subsequently, 150 µl of culture supernatants were collected at 5 dpi, and the viral RNA load was examined by real-time RT-PCR, as described in section 2.9.

2.5. Expression of rGP and pseudotype virus production

The open reading frames for the KHF4 and KHF5 GPs were amplified from viral complementary DNA (cDNA) using the following primer pairs: KHFV_M41F_EcoRI (5′-ATCGAATTCATGGGGATATGGAAGTGGCTAGTGATG-3′) and KHFV_M2450R (5′-TCCTGCTATACCTTATTGTGATG-3′), and KHFV_2250F (5′-GTGCTTGTACAAAGTATGAATAACC-3′) and KHFV_M_M3448R_XhoI (5′-AGCCTCGAGCTATGACTTTTTATGCTTCTTTACGG-3′). The entire open reading frame was connected by overlapping PCR and inserted into the *Eco*RI and *Xho*I sites of the mammalian expression vector pCAGGS/MCS. The sequences of the final plasmid constructs pCAG-KHF4M and pCAG-KHF5M were confirmed by Sanger sequencing. The plasmid vectors were transfected into Vero E6 cells to analyze their antigenicity. The plasmids were also transfected into 293T cells to propagate the pseudotype vesicular stomatitis virus (VSV) coated with recombinant GPs of KHF4 and KHF5, as described previously[60]. The titers of the pseudotype viruses VSVΔG*-KHF4 and VSVΔG*-KHF5 were counted as the number of green fluorescent protein signals in Vero E6 cells.

2.6. Western blot

Cell monolayers in 6-well plates were inoculated with KHF4 and KHF5 at MOI =0.1. Five days after inoculation, the cells were lysed with 200 µl SDS sample buffer and heated to 100 °C for 10 min. The lysate (15 µl) was loaded onto an SDS PAGE

gel (e-PAGEL 1020 L, Atto, Tokyo, Japan) and electroblotted onto a 0.45 μm pore immunoblot PVDF membrane (Millipore, Billerica, MA, USA). The N protein of HTNV was detected using the rabbit polyclonal antibody targeting the recombinant N protein of HTNV[63], and a horse radish peroxidase (HRP)-conjugated goat anti-rabbit IgG antibody (Jackson Immuno Research Laboratories Inc., Baltimore, MD, USA, 111-035-003). Bound antibodies were reacted with Amersham ECL Prime (Cytiva, Tokyo, Japan) and detected using an ImageQuant LAS 4000 mini (Cytiva).

2.7. Animal experimentation

Five-week-old female BALB/cCrSlc mice (SLC, Hamamatsu, Japan) were injected with 10^5 focus forming units (FFU) of KHF4 or KHF5 via the tail vein. The weights of the mice were measured from 1 to 14 dpi. At 1, 3, 5, and 7 dpi, two animals were euthanized, and blood was collected. If available, urine samples were collected. The lungs, kidneys, spleens, and livers were collected and stored at −80 °C for RNA extraction and viral protein detection. Tissue pieces from the lungs were used for further cultivation to analyze viral replication. Mouse organs were fixed in 4% phosphate-buffered paraformaldehyde (Fujifilm Wako) for histological analysis. All animal experiments were approved by the Animal Studies Ethics Committee of Hokkaido University (19-0088). The mice were treated according to the laboratory animal control guidelines of the Hokkaido University Institutional Animal Care and Use Committee. Experiments involving viral infections were performed at a BSL-3 facility.

2.8. Viral replication in lung tissues ex *vivo*

Lungs were obtained from mice and cut into four pieces. The lung pieces were cultivated in the upper chamber of the culture insert (1 μm pore size, Corning 35310, New York, NY, USA) in 24-well plates using DMEM supplemented with 10% FBS and antibiotics. Briefly, 10^6 FFU of the KHF4 and KHF5 viruses were inoculated into the lung pieces which were subsequently incubated in 5% CO_2 at 37 °C. At 24 h after inoculation, the medium was replaced with fresh medium. After 7 days of inoculation, culture medium from the lower chamber was collected, and viral load was analyzed by real-time RT-PCR as described in section 2.9. Next, lung tissues were obtained from KHF4- and KHF5- infected mice and were cultivated as described. After 7 days of incubation, the culture medium from the lower chamber was collected, and the viral load was analyzed as described.

2.9. RNA extraction and real-time RT-PCR

Total RNA was extracted from each tissue using ISOGEN (Nippon Gene, Tokyo, Japan), as per the manufacturer's protocol. Real-time RT-PCR was performed using the iTaq Universal SYBR Green one-step kit (Bio-Rad Laboratories, Richmond, CA, USA). The qPCR primer sets used were KHFV-SF (5′-TGGACCAAAGGATTATTGTGC-3′) and KHFV-SR (5′-CATCCCCTAAGTGGAAGTTGTC-3′). The mouse β2-microglobulin forward (5′-ACAGTTCCACCCGCCTCACATT-3′) and reverse (5′-TAGAAAGACCAGTCCTTGCTGAAG-3′) primer pair were used to measure the standard gene to compare cell numbers.

2.10. Viral antigen detection in organs

Approximately 10 mg of tissue was lysed in 200 µl SDS sample buffer and heated to 100 °C for 10 min. The lysate (15 µl) was loaded onto an SDS PAGE gel and viral N protein was detected by western blotting as described in section 2.6 (page 17). HRP-conjugated anti-GAPDH antibody (Proteintech, Rosemont, IL, USA, HRP-60004) and anti-β-actin antibody (Sigma-Aldrich, A5316, Merck) was used to adjust the total protein concentration in the lysate.

2.11. Histopathology and IHC

Tissues were fixed in 4% paraformaldehyde phosphate buffer solution (Fujifilm-Wako) at 4 °C, embedded in paraffin within 14 days, sectioned, and stained with hematoxylin and eosin (HE) (Sapporo General Pathology Laboratory, Sapporo, Japan) to detect the N antigen of KHFV, using the biotinylated E5/G6 monoclonal antibody[88]. Immunohistochemistry (IHC) was performed using the Vector M. O. M. immunodetection kit (Vector Laboratories, Burlingame, CA, USA) following the manufacturer's protocols.

2.12. Microarray analysis

KHF4, KHF5, and mock-infected mouse livers were collected and stored in RNA Later (Invitrogen). RNA was extracted as described previously, and gene transcription in the liver was analyzed via microarray analysis, performed at GeneticLab Co. Ltd (Sapporo, Japan). Briefly, extracted RNA was treated using a GeneChip WT Pico Reagent kit (Applied Biosystems) according to the manual instructions and then hybridization was performed using Clariom S Array for mice (Applied Biosystems). Data were analyzed using Transcriptome Analysis Console (TAC) (Thermo Fisher Scientific).

2.13. White blood cell population

A blood smear was prepared to examine the white blood cell (WBC) population. After fixing with methanol for 10 min, slides were stained with Giemsa solution. A total of 400 white blood cells were counted on each slide, and the numbers of monocytes, neutrophils, and lymphocytes were recorded. To count the white blood cell number, 2 µl of blood was mixed with Turk stain solution (Nacalai Tesque), and the WBC numbers were counted under a microscope.

2.14. Clinical pathology of infected mice

Serum alanine transaminase activity was analyzed as an indicator of liver dysfunction using a serum alanine transaminase (ALT) colorimetric activity assay kit (Cayman Chemical, USA). Blood urea nitrogen (BUN) levels were analyzed as an indicator of renal dysfunction (DetectX Urea Nitrogen Colorimetric Detection Kit, Funakoshi, Tokyo, Japan). Urinary proteins were analyzed by SDS-PAGE, followed by protein staining (Simply Blue, Invitrogen, Thermo Fisher Scientific). IL-6 and tumor necrosis factor (TNF)-α levels were evaluated to detect the systemic cytokine storm using a mouse IL-6 detection kit (Chondrex #6702, USA) and mouse TNF-α detection kit (Chondrex #6701), respectively, following the manufacturer's protocols.

2.15. Statistics

The paired student's *t*-test was used, and statistical significance was set at $p < 0.05$. Significance was assigned as * $p < 0.05$, ** $p < 0.01$, and *** $p < 0.001$. Images of Western blot bands yielded by anti-N antigen and GSPCF antibodies were quantified using open-source Fiji/Image-J software (https://*doi*.org/*10.1038*/*nmeth.2019*)[69].

3. Results

3.1. Characterization of KHF4 and KHF5 GPs

The amino acid at position 417 in the GP is the sole difference between the viral proteins of KHF4 and KHF5, and the amino acid may be responsible for virulence in mice. However, the role of this substitution has not been clarified. To investigate the role of this mutation, we compared the antigenicity, fusion activity, and growth of the two viruses and their recombinant GPs. First, antigenic profiling using 23 types of monoclonal antibodies against the HTNV GP indicated no remarkable antigenic difference between the KHF4 and KHF5 GPs (Fig. 2A), KHF4 and KHF5 inoculated and rGP-expressing Vero E6 cells were exposed to low pH. As shown in Fig. 2B, both KHF4 and KHF5 showed high cell fusion activity. Next, viral replication was analyzed in Vero E6 cells. KHF4 and KHF5 were inoculated into Vero E6 cells at an MOI of 0.1, and the supernatant was collected from 1 to 10 dpi to determine the amount of viral RNA present using real-time RT-PCR (Fig. 2C). The viral RNA copy number of KHF5 was significantly higher than KHF4 since 3 dpi. To compare viral entry, pseudotype VSV coated with the rGPs of KHF4 and KHF5 were generated (Fig. 2D). Both pseudotyped viruses showed high and similar titers. This observation indicates that both GP were assembled into VSV virions without any difference.

A

Monoclonal antibodies	Epitope	KHF4	KHF5
8B6	Gn a	++	++
6D4		++	++
10F11		++	++
2D5	Gn b	++	++
3D5		+	+
16D2		++	++
HCO2	Gc a	+++	+++
16E6		++	++
EBO6	Gc b	+	+
11E10 2-2	Gc c	+++	+++
17G6	Gc e	++	++
3D7		++	++
5B7		++	++
20D3		++	++
8E10	Gc f1	++	++
1C6		++	++
1G8		+++	+++
23G10-2		++	++
3B6		++	++
23G10-1	Gc f2	+	++
7G6		++	+
18F5		++	++
E5/G6	N	+++	+++

B

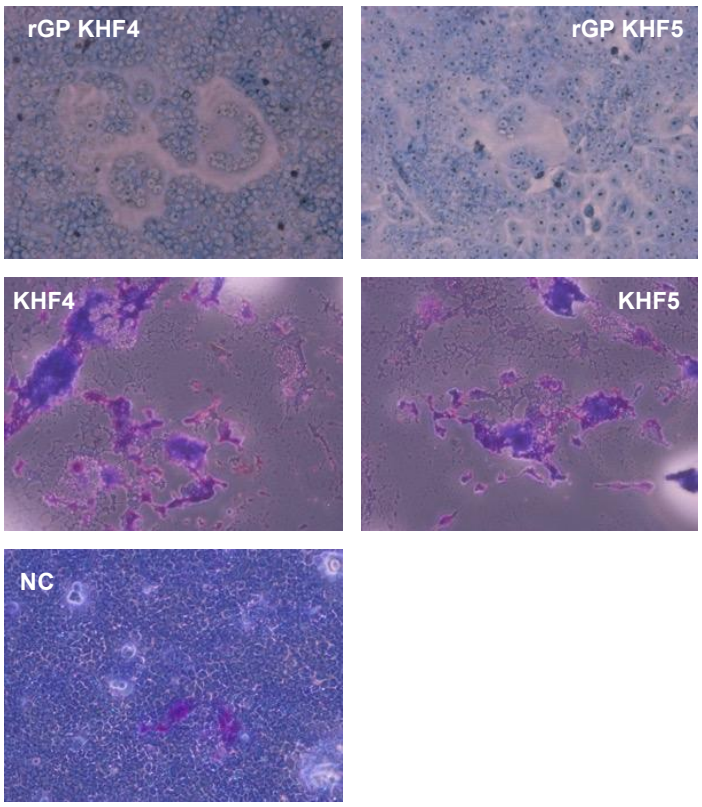

C

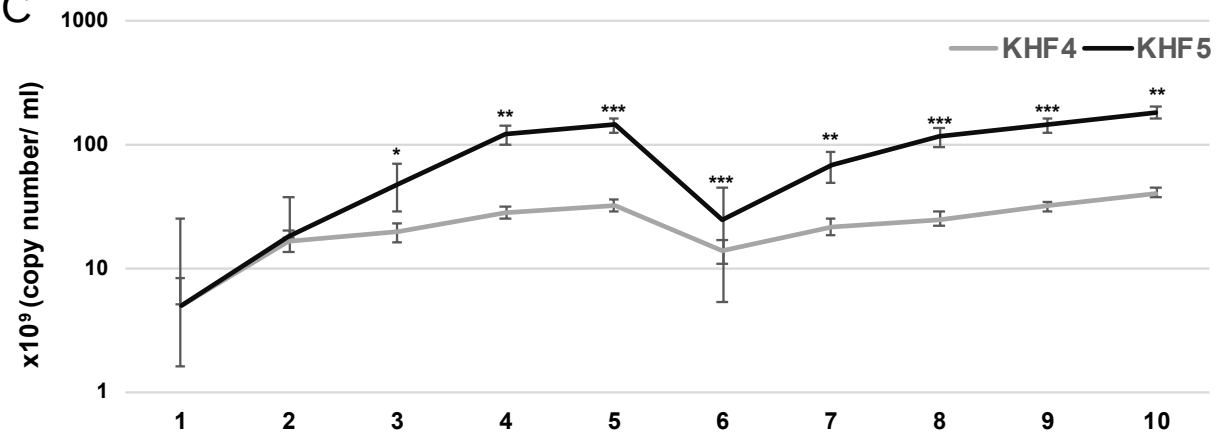

D

Pseudotype virus	VSVΔG*-KHF4	VSVΔG*-KHF5
Titers (FFU/ml)	4.2 x 10^5	7.1 x 10^5

Figure 2 Virological characterization of KHF4 and KHF5.

(**A**): GPs of KHF4 and KHF5 were compared for monoclonal antibody binding. The culture supernatants of hybridoma of monoclonal antibodies were diluted 1:1, 1:10, and 1:100, and positivity in the 1:100, 1:10, and 1:1 dilution was assessed as +++, ++, and +, respectively.

(**B**) Cell fusion assay. Cell fusion activity of recombinant glycoproteins of KHF4 and KHF5 expressed in Vero E6 cells by transfection (upper panels). Fusion activity of Vero E6 cells infected with KHF4 and KHF5 (central panels). Cells were inoculated with viruses at a MOI of 0.1 and incubated for 5 days. Uninfected Vero E6 cells were used as negative controls (NC; lower panel).
(**C**) Viral growth in Vero E6 cells. Culture supernatant was collected from cells between 1 to 10 dpi, and the viral load was quantified by real-time RT-PCR.
(**D**) Pseudotype VSV were infected to KHF4 and KHF5 glycoproteins expressing HEK293T cells and the propagated pseudotype VSV and titers were determined in Vero E6 cells.

3.2. The cell tropism of KHF4/KHF5 *in vitro*

To identify the factors responsible for the virulence change caused by the E417K mutation, the cell and organ tropism of KHF4 and KHF5 were examined in *vitro*. As shown in Fig. 3, the production of viral N protein after inoculation with KHF4 and KHF5 was compared in Vero E6, A549, U937, and HEK 293T cells. KHF4 showed higher N protein production than KHF5 in all cell lines except U937. Vero E6 cells were used for amplification of HTNV strain 76–118. A549 cells were originally used for amplification of HTNV 76–118[46]. Conversely, U937 cells were used for antibody dependent enhancement of HTNV 76–118[82], meaning that without anti-GP antibodies, U937 cells were not infected with HTNV 76-118. Similarly, KHF4 and KHF5 had no infectivity to U937 cells in the current experiments. In mouse in *vitro* experiments, KHF4 showed higher N protein production than KHF5 in peritoneal macrophages, dendritic cells, and splenocytes, similar to in the cell lines. Compared with the prototype HTNV strain 76–118, which was not pathogenic in immunocompetent mice, both KHFV strains showed high infectivity toward immune cells.

According to the observations from Vero E6 cells shown in Fig. 1C and Fig. 2A, KHF4-infected cells expressed N protein in cells more than KHF5-infected cells; however, virus release was significantly lower than in KHF5-infected cells. The tendency of intracellular N protein to be higher in KHF4-infected cells is consistent in various cells shown in Fig. 3. The results suggest slight differences between KHF4 and KHF5 in the release of viral progeny. Next, I needed to examine differences between KHF4 and KHF5 in mice to understand KHF5 pathogenesis.

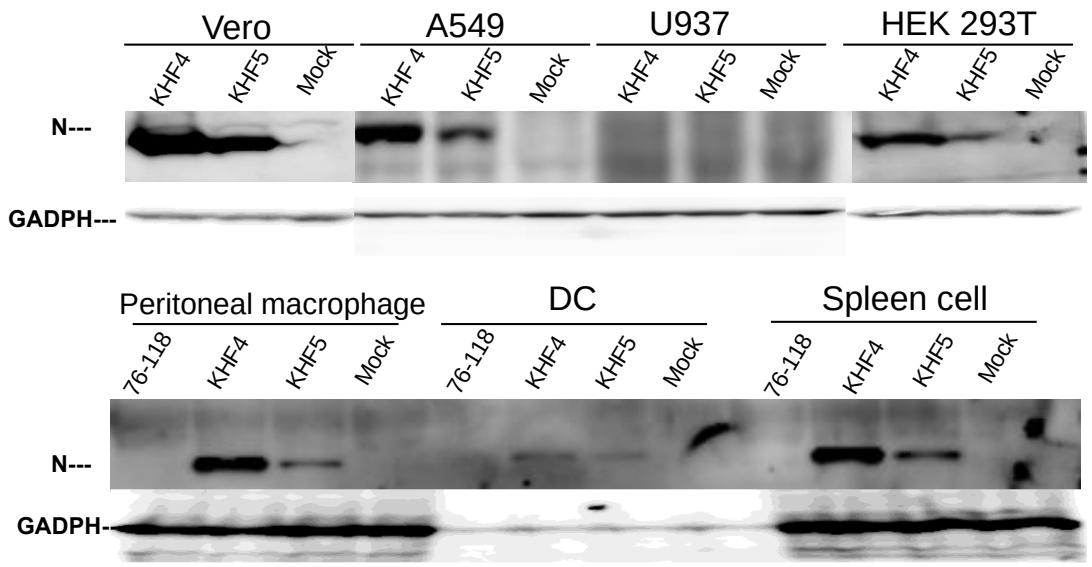

Figure 3 Cell tropism of KHF4 and KHF5 *ex vivo*

Viral N protein production was compared by Western blotting to clarify virus replication in various cells. Four cell lines, (Vero E6, A549, U937, and HEK 293T) and peritoneal macrophages, dendritic cells (DC), and spleen cells obtained from five-week-old BALB/c mice were inoculated at a MOI of 0.1 and cultured for 5 days. GAPDH was used as the reference protein.

3.3 KHF5 targeting the lungs may play an essential role in pathogenesis

As reported previously, BALB/c mice infected with KHF5 showed weight loss at 5 dpi (Fig. 4A) [71], and severe kidney hemorrhage occurred at 7 dpi (Fig. 4B), from which the mice subsequently clinically recovered, based on symptoms such as ruffled fur and decreasing activity. As shown in Fig. 4A, the viral RNA loads in the lung, liver, spleen, and kidney were determined at 1,3, 5, and 7 dpi using real-time RT-PCR. The viral RNA load in the lung and kidneys was significantly higher in KHF5 than in KHF4-inoculated mice at 3 dpi. In the lungs, high levels of viral N protein were detected in mice with KHF5 infection alone (Fig. 5B). The results suggest that the lungs are an important site for viral replication during the early phase of infection in mice. A high viral load in the liver was detected in both the KHF4 and KHF5-inoculated mice. Significantly higher viral loads were observed in KHF5-inoculated mice at 5 and 7 dpi. Viral N protein was detected in the liver, and the ratio of protein was almost the same as that in the lung when compared with the reference protein GAPDH in KHF5-infected mice (Fig. 5C). Conversely, in KHF4-infected mice, N protein production in lung was lower than in KHF5-infected mice. The results suggest that the high viral load in KHF5 infected lung at the early phase may related to the renal hemorrhage appearance. Viral N protein in spleens were below detectable levels.

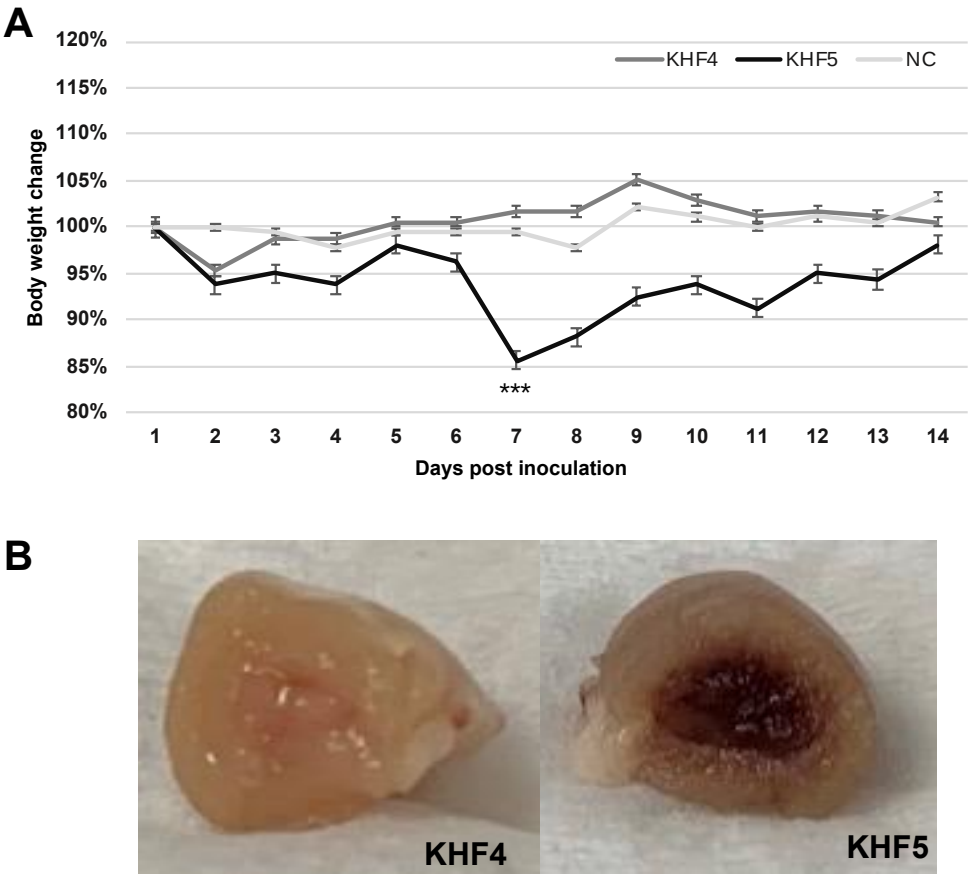

Figure 4 Body weight and renal changes in mice with KHF4 and KHF5 infection.

(**A**) Five-week-old BALB/c mice were infected with KHF4 and KHF5 strains, or mock inoculation with culture medium of Veo E6 cells (NC). Subsequently the weight changes were measured between 1 to 14 dpi. (**B**) At 7 dpi, a significant weight loss and renal hemorrhage were observed.

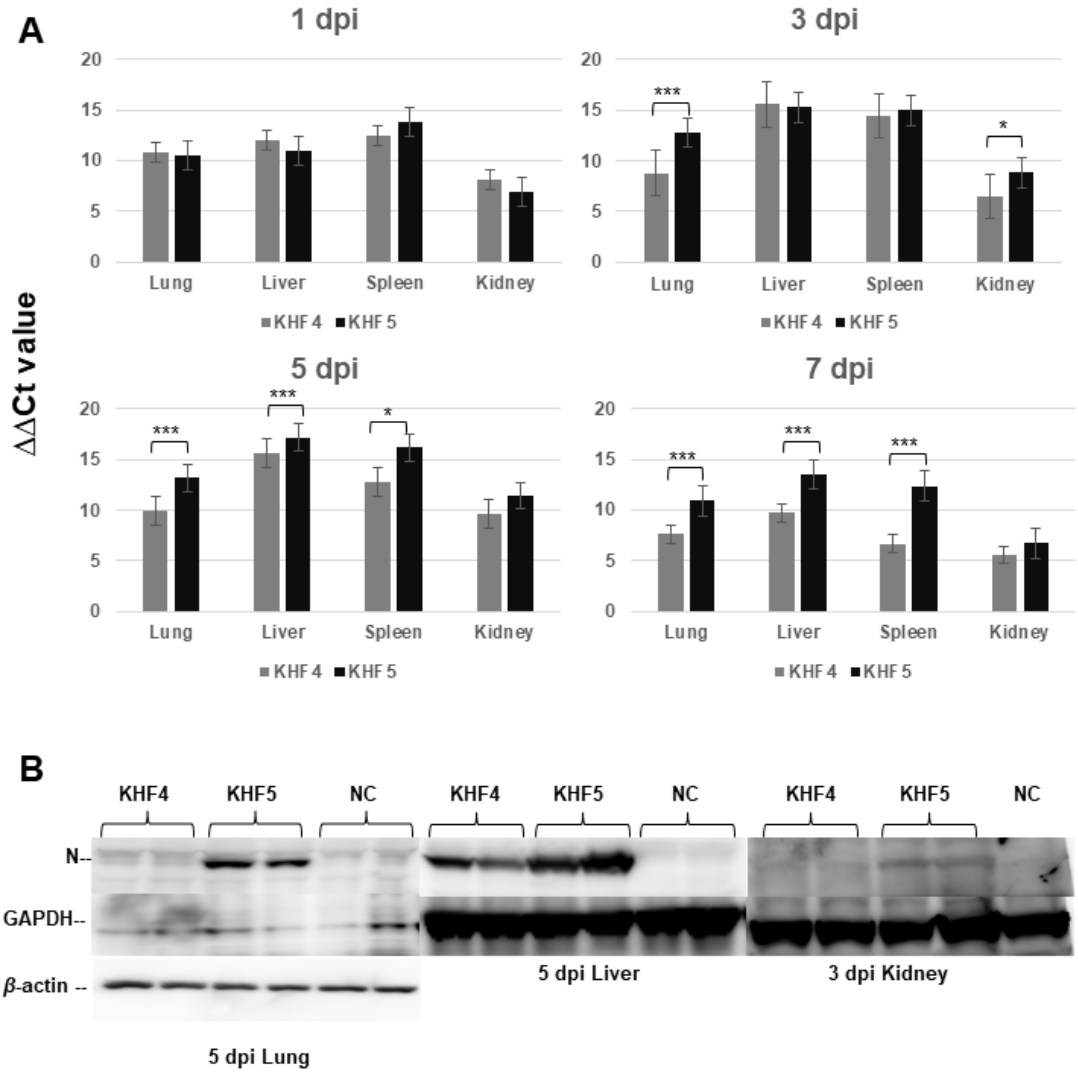

C

	N protein / GADPH	
Mouse ID	**Lung**	**Liver**
KHF4 #1	0.13	1.12
KHF4 #2	0.44	1.11
KHF5 #1	1.95	1.73
KHF5 #2	1.67	2.17
NC #1	0.00	0.04
NC #2	0.02	0.05

Figure 5 Viral replication in the lung, liver, spleen, and kidneys.

(A) Viral load in the four organs were quantified via real-time RT-PCR. The viral load was detected using S segment primer sets, normalized relative to β-2 microglobulin, and compared with the negative control ($\Delta\Delta$Ct KHFV = (Ct $_{KHFV\ S}$ – Ct $_{KHFV\ \beta 2M}$) – (Ct $_{NC\ S}$ – Ct $_{NC\ \beta 2M}$)). (**B**) The anti-HTNV viral N protein was detected by western blotting. Results from each two mice are shown. **(C).** Western blot images of lung and liver shown in Fig. 4B were quantified by Fiji/ImageJ software. Ratio of N protein to GAPDH was estimated in liver and lung tissues.

3.4. Viral replication in the lung tissue

To confirm the KHF5 tropism in the lungs, lung tissues from infected mice were cultured. After 7 days, culture supernatants were collected from the lower chamber and viral load was examined by RT-PCR. Viral RNA load in the medium were higher for KHF5 than KHF4 (Fig. 6A). Next, KHF4 and KHF5 were inoculated into the lung tissue obtained from mice with no viral inoculation, and the tissues were subsequently cultured for 7 days (Fig. 6B). KHF4 showed higher viral production in the culture supernatant and N protein production in the lung tissue than KHF5 (Fig. 6C).

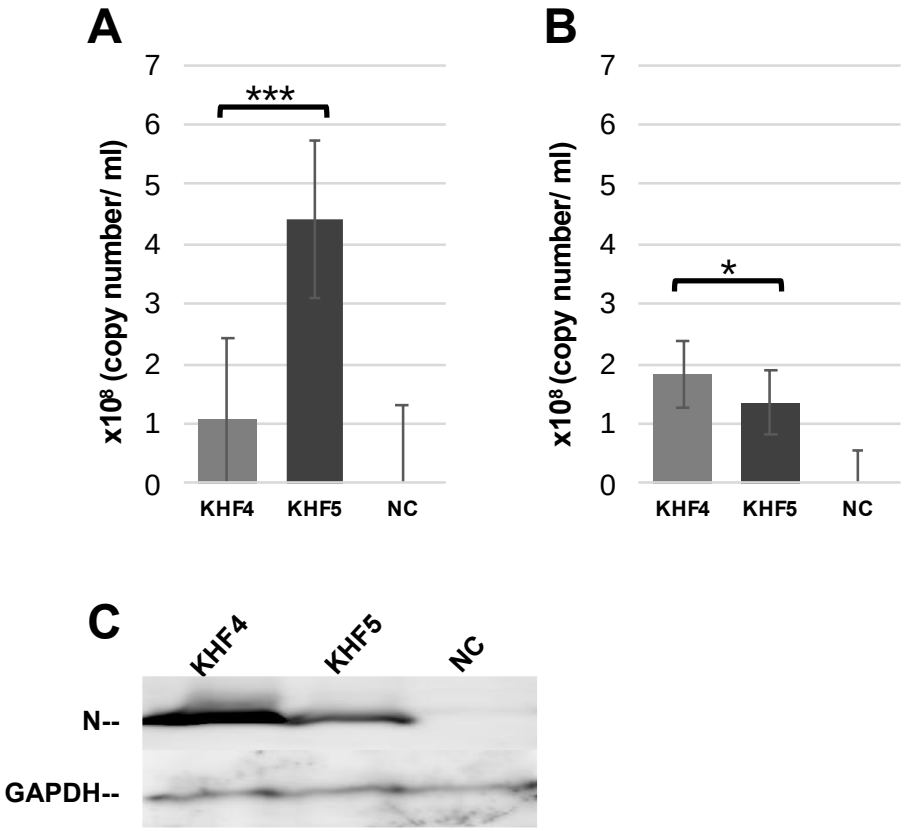

Figure 6 KHF4 and KHF5 replication in lung tissue.

(A) Lungs were collected from KHFV-infected mice at 5 dpi and cultured. After 7 days, the supernatant was collected for real-time RT-PCR. (**B**) Uninfected BALB/c mouse lungs were collected and cultured as described above. After infection with KHFV, the supernatant was collected at 7 dpi for real-time RT-PCR analysis. (**C**) Viral N protein in the lung tissue as shown in Fig. 5B detected by western blot. Results from mock inoculated mouse and lung tissue are shown in NC.

3.5. KHF5 infection caused renal hemorrhage, lung edema, and acute hepatitis

As reported previously[71], KHF5 infection causes renal hemorrhage. As KHFV targeted the lungs and both strains showed high infectivity to the liver, viral N antigens were analyzed by IHC to examine the distribution of viruses in the lung, liver, and kidneys. In the KHF5-infected lungs of mice, viral antigens were detected in alveoli and bronchial epithelial cells, compared with the negative control and KHF4 infected lungs. KHF5 infection caused severe pneumonia, and aggregation of lymphoid cells was identified near the peri-bronchus edema. Additionally, mononuclear cell infiltration with KHFV antigens was found in capillary vascular endothelial cells (Fig. 7A). As both strains showed high infectivity in the liver, the viruses caused acute hepatitis due to lymphocytic infiltration of inflammatory cells. Reduced glycogen storage and petechial hemorrhage were observed in KHF5-infected mice alone (Fig. 7B). Focal interstitial hemorrhage was observed in the renal medulla, cortex, and tubular region in KHF5-infected mice alone, and viral antigens were detected mainly in the tubular region (Fig. 7C).

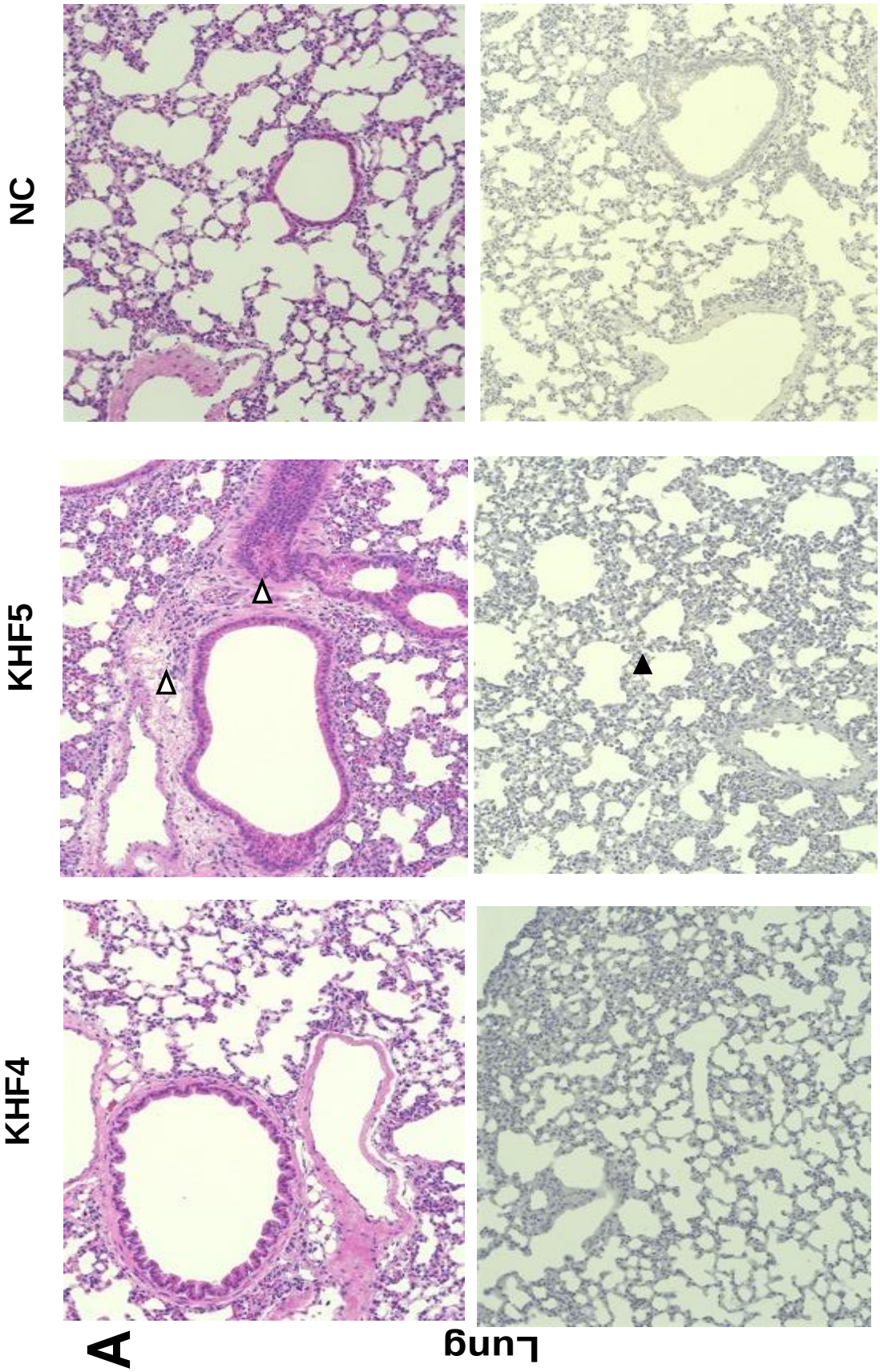
NC
KHF5
KHF4
A
Lung

B
Liver
NC
KHF5
KHF4

NC
KHF5
KHF4
C
Kidney

Figure 7 Immunohistochemistry analysis of tissues from KHF4 and KHF5-infected mice

Tissue slices were stained with hematoxylin and eosin (HE), and viral antigens were detected using a biotinylated E5G6 monoclonal antibody with the Vector M.O.M immunodetection kit. Characteristic lesions were indicated by open triangles. Viral antigens are indicated by closed triangles. (**A**) Peri bronchus edema with lymphocyte aggregation was observed in KHF5-infected lungs, and mild antigen reaction was observed in KHF5-infected alveolar epithelial cells. (**B**) Petechial hemorrhage was observed in KHF5-infected livers by HE staining, whereas KHF5-infected livers showed multiple antigenic reactions and hemorrhage. The KHF4 infected liver also showed perivascular lymphoid infiltration. (**C**) Renal hemorrhage caused by KHF5 infection was distributed in the cortex-medullary region, and antigens were detected in the tubular regions.

3.6. KHF5 infection caused acute hepatitis and neutrophilia

Acute hepatitis with lymphocytic infiltration of immune cells was observed in the KHF4 and KHF5 sections; therefore, liver dysfunction was assessed via ALT activity analysis. As shown in Fig. 8A, serum ALT activity was significantly increased in both KHF4 and KHF5-infected mice at 7 dpi. In contrast, BUN levels did not change at 5 dpi and 7 dpi despite renal hemorrhage (Fig. 8B). We collected blood from each mouse at 1, 3, 5, and 7 dpi to examine the white blood cell population levels, which showed a decrease in white cell numbers at 5 dpi, and an extreme increase at 7 dpi. At 5 dpi, KHF5-infected mice showed a high ratio of neutrophils, indicating that neutrophilia may be related to pathogenesis in this phase (Fig. 8C). Serum IL-6 and TNF-α were examined but both of them were not detected (Figure 9A). To analyze renal damage, we examined renal proteins by SDS-PAGE (Figure 9B). Compared to urine from control mice, multiple bands were evident in the urine of infected mice, indicating that functional changes may have occurred. However, albuminuria was not detected. Notably, 120 KDa bands were observed in KHF5 inoculated mice at 7 dpi, though the protein sequences could not be identified (data not shown). Urine kidney injury molecule (KIM-1) levels were also examined using a KIM-1 detection kit, but no increase in KIM-1 levels was detected (data not shown).

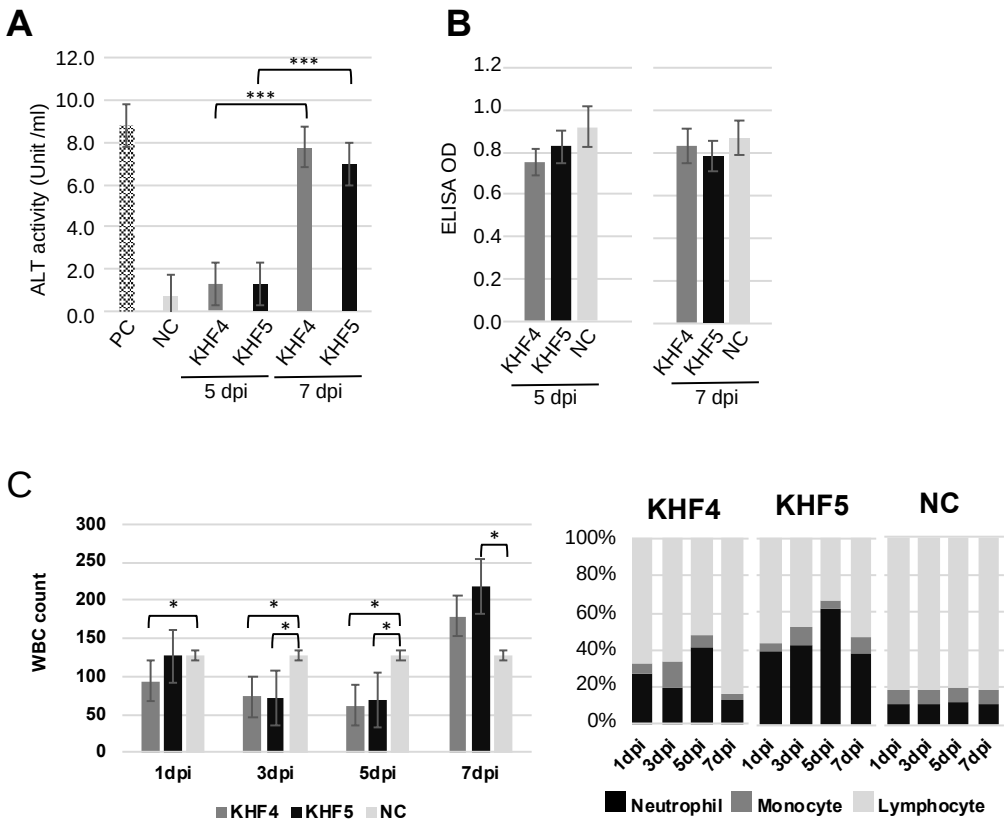

Figure 8 Clinicopathological tests by peripheral blood and serum.
(**A**) Fluctuation of ALT for liver dysfunction. (**B**) Fluctuation of BUN. MEM medium injected into five-week-old BALB/c mice was used as the negative control (NC), and the positive control (PC) was provided with an ALT kit. The optical density was read at 340 nm and 450 nm, and ALT activity and BUN analysis were performed as per the manufacturer's instructions. (**C**) White blood cell number per µl of blood (left panel) and in the population (right panel).

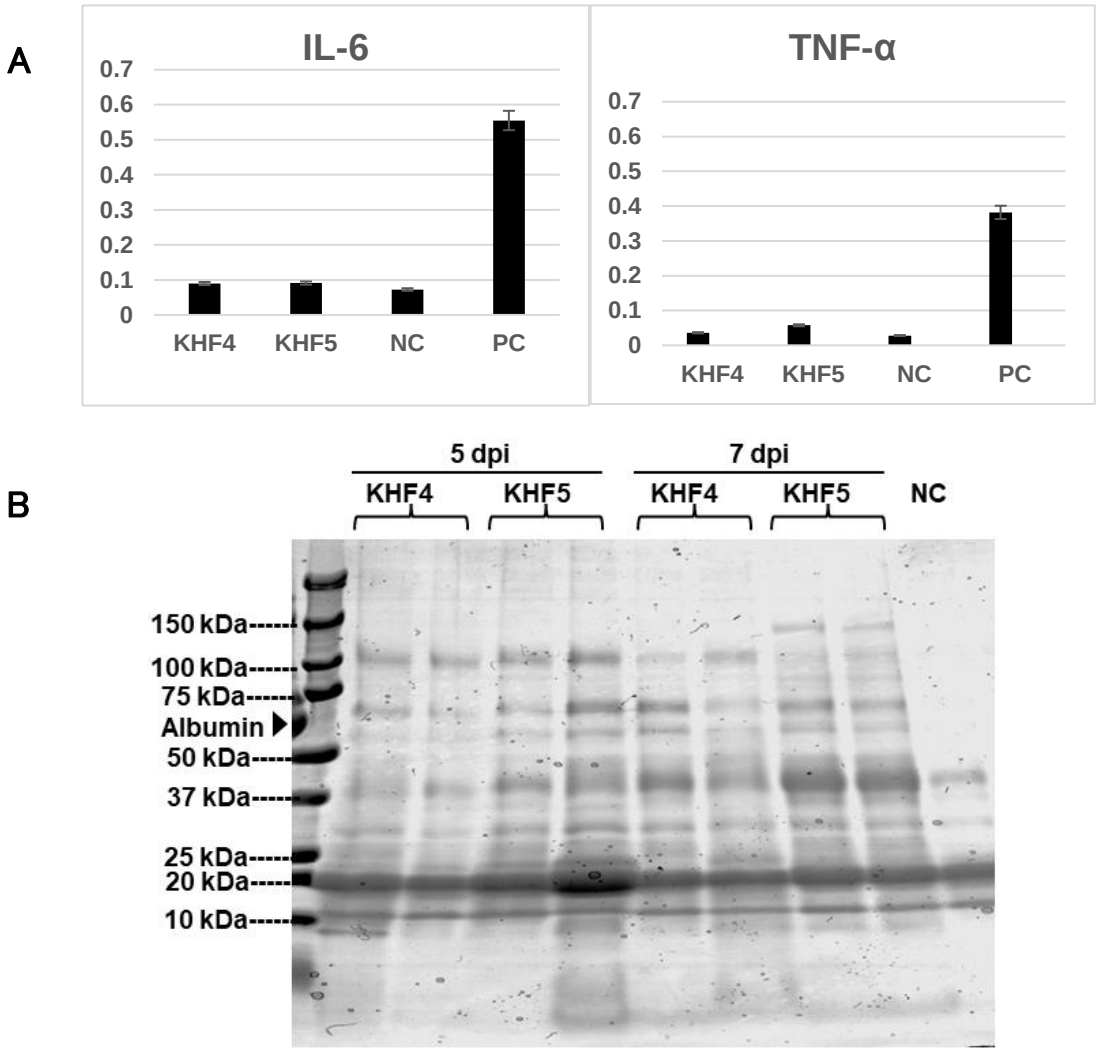

Figure 9 Detection of serum cytokine concentration and detection of protein urea in KHF4 and KHF5 inoculated mice

A). Comparing the IL-6 and TNF-alpha levels in sera. Sera were obtained from KHF4, KHF5 at 7 dpi, and mock infected mice (NC, n=2). Sera were examined at 1:3 dilutions. Positive control IL-6 (333.3 pg/ml) and of TNF-alpha (187.5 pg /ml) were used. All tests were performed in duplicate.

B). Urinary protein analysis by SDS-PAGE. Urine from KHF4 and KHF5 infected and non-infected mice were applied to gels at 10 ul / lane.

3.7. KHFV infection induces T cell and neutrophil infiltration in the liver

I found that KHF4 and KHF5 show high levels of replication in the liver and cause hepatitis. To analyze the pathogenicity of these viruses in the liver, mRNA expression was examined using microarray analysis. A total of 20,226 genes showing transcriptional changes were compared among the KHF4, KHF5, and mock infection groups. As shown in Fig. 10A, the expression of several genes was altered between the infected and control groups. However, few genes differed in expression between the KHF4 and KHF5 groups. Increased expression of genes in CD8+ T cells and that of licocalin-2 was identified in both KHF4 and KHF5-infected liver cells. As shown in Fig. 10B, the levels of cytotoxic T cell (granzyme A and B) and neutrophil-related genes (lipocalin-2/neutrophil gelatinase-associated lipocalin) were increased. In KHF4-infected mice, the expression of CD8+ cell-related genes showed a greater increase than in KHF5-infected mice. In contrast, lipocalin-2 expression levels were changed in KHF5-infected mice more than in mice infected with KHF4. These genes were derived from cells that infiltrated into the liver from the blood or hepatocytes. In contrast, acute phase proteins produced by hepatocytes (serum amyloid A2 and A3) were higher in both KHF4 and KHF5-infected mice, indicating that viruses induce inflammation in the liver, but KHF5 may cause a predominant response to neutrophils.

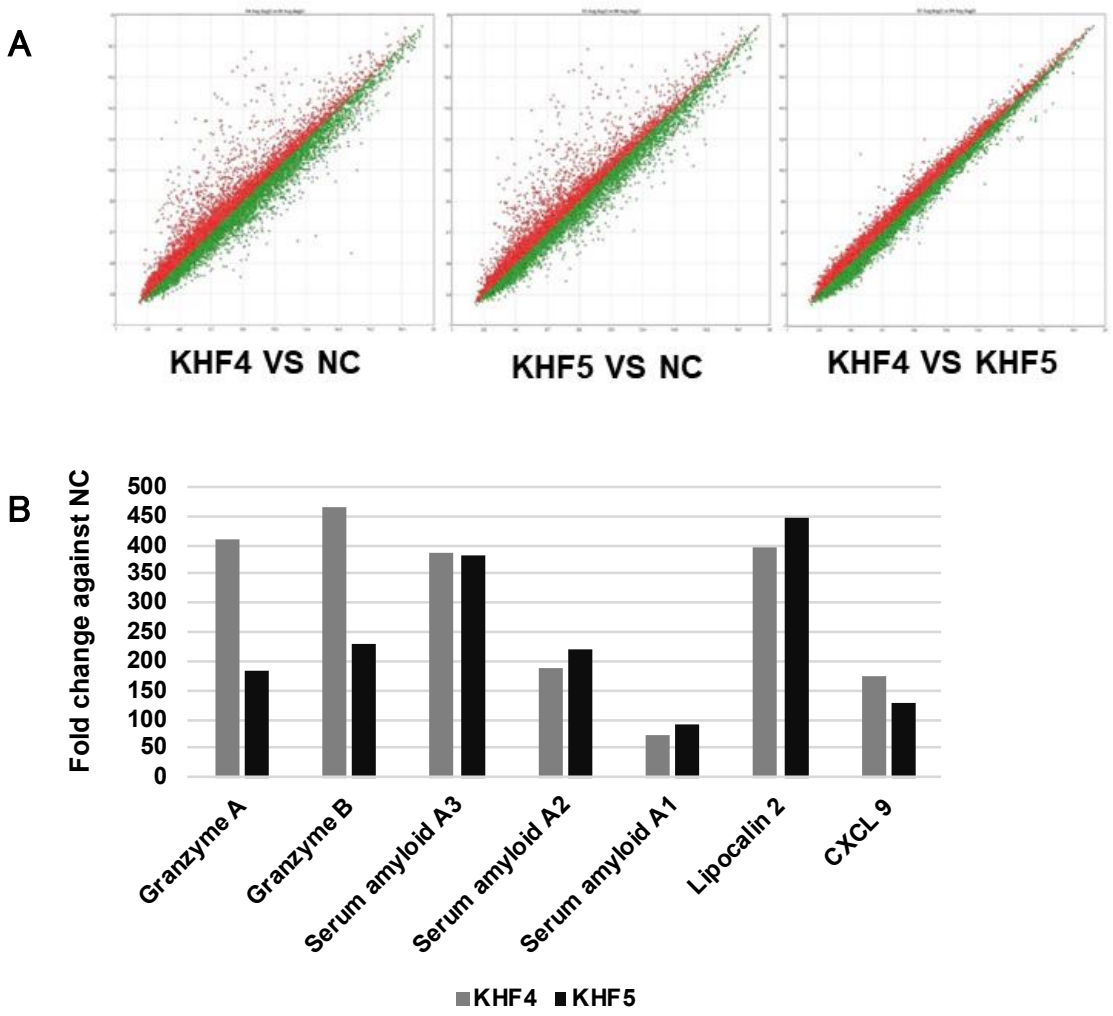

Figure 10 Liver gene expression profiling using microarrays.

A). Transcriptional changes were compared between the three groups. The scatter plot shows the transcript clusters, and a total of 22,206 transcript clusters were analyzed. **B).** Transcriptional changes were compared in KHF4, KHF5, and mock-infected mice. The top ten genes showing the maximum fold-change difference in KHF4/KHF5-infected mice relative to the controls were selected and compared.

4. Discussion

In this study, KHF5 was used to investigate HFRS-like pathogenesis in mice. It was previously reported that the amount of viral RNA in the kidneys of KHF5-infected mice was greater than that in KHF4 infected mice and peaked before the onset of disease[71]. However, the organ tropism and histological data were not fully examined to evaluate whether this experimental mouse was suitable as a model for human HFRS. Therefore, the renal pathology was analyzed in this study. The viral antigen and petechial hemorrhage were identified in the tubular region, which induced HFRS symptoms in humans[23].

In addition, I found that the pathogenic strain KHF5 alone targeted the lungs and caused lung edema in the HFRS mouse model. The high viral load detected from KHF5 infected lungs at the early phase may suggested the relationship to renal hemorrhage appearance. We also found neutrophil infiltration near the bronchus edema. Previously, we reported that the depletion of neutrophils can suppress pulmonary vascular hyperpermeability and the occurrence of pulmonary edema in SCID mice[39]. In humans, a few HFRS patients reportedly develop respiratory disorders[16,66]. Inhalation of excreta from wild rodents is considered the main route of hantavirus transmission to humans, and an epidemiological study on the Puumala virus (PUUV), one of the causative agents of HFRS in Europe, indicated a relationship between smoking and seropositivity[43]. Burdening the lungs by smoking can increase the efficiency of hantavirus infection. These reports suggest that the lungs play an essential role as the primary target site in the initial phase of hantavirus infection.

Interestingly, both strains showed extremely high infectivity towards the liver, and acute hepatitis and lymphatic infiltration of inflammatory cells were observed in KHF4 and KHF5-infected mice. The elevated ALT levels showed KHF viruses caused

acute hepatitis in mice. Serum ALT activity and liver section analysis showed that KHF4 and KHF5 infections caused hepatitis; however, glycogen storage reduction and petechial hemorrhage in the presence of viral antigens were detected in mice with KHF5 infection. Significant increases in ALT activity have been frequently reported in HFRS cases, and liver damage is considered important for hantavirus pathology [59,77].

We counted the number of white blood cells in mice at 1, 3, 5, and 7 dpi, and found that leukocyte levels decreased from 3 to 5 dpi and were subsequently increased at 7 dpi, which was similar to the pattern observed in two patients with severe HFRS infection as reported previously[41]. In addition, Strandin and colleagues reported the presence of neutrophil activation in acute HFRS[74]. A similar increase in neutrophils was observed in KHF5-infected mice at 5 dpi, the onset points of weight reduction and renal hemorrhage, and the levels were subsequently reduced at 7 dpi at a severe stage of disease which was considered to indicate the beginning of recovery. The change in neutrophil levels followed by the change in symptoms indicates the importance of neutrophils in HFRS pathogenesis.

Cytokine storms may play a crucial role in the manifestation of both HFRS and HPS[22,36]. To examine the cytokine storm in mice, the levels of IL-6 and TNF-α in the blood at 7 dpi were analyzed, but no significant differences were found among the KHF4, KHF5, and negative control groups. Therefore, a systemic cytokine storm was not considered to have occurred in these mice.

The microarray analysis results showed that both KHF4 and KHF5 showed high expression levels of granzyme A and granzyme B in the liver, which were produced mainly by CD8+ T cells. Recently, we reported that CD8+ T cells are involved in the development of renal hemorrhage in KHF5 inoculated mice[72]. Notably, non-pathogenic KHF4 induced higher expression of granzyme A and B than KHF5. These

results suggest that CD8+ effector T cells may be involved in renal injury and recovery from infection. Lipocalin-2 expression showed a 393-fold and 445-fold increase in KHF4 and KHF5-infected mice, respectively, compared to the negative control group. Lipocalin-2 is mainly expressed by neutrophils and hepatocytes and is induced by IL-6 in mice[80]. In this study, the source of lipocalin-2 in the infiltrated neutrophils or hepatocytes was not determined. However, the increase in lipocalin-2, serum amyloid A2, and A3 gene expression levels in the microarray analysis indicated the induction of inflammatory cytokines in the liver. An increase in BUN levels or albuminuria were not observed in KHF4 and KHF5 inoculated mice, despite the presence of renal hemorrhage. It was difficult to collect enough volumes of urine specimens to examine KIM-1 from mice. In HFRS patients, KIM-1 elevation in urea was reported[26]. In the present study, KIM-1 concentrations in a few urine samples were examined; however, we could not detect high concentrations of KIM-1. Further investigations are required to evaluate renal dysfunction in KHF5-infected mice.

Hantavirus is beginning to be recognized as a virus that causes hepatitis[79]. Recently, it has been reported that the livers of host rodents are infected with hantaviruses[27]. Seoul orthohantavirus targets the microvasculature in the liver of chronically infected asymptomatic rats[54]. In the present study, KHF5 could infect parenchymal cells of the liver more frequently than endothelial cells. Moreover, antigen-positive hepatocytes were dispersed. However, there are very few reports on hantavirus infectivity to hepatocyte. Once the types of hepatocytes targeted by hantavirus in the liver are known, novel techniques such as single-cell RNA sequencing, would provide useful information.

As demonstrated in a previous paper, under KHF5 infection, T-cells are obviously involved in the expression of pathogenicity, because weight loss was not

observed following CD8+ T cell depletion[71,72]. Results from microarray analysis of liver also suggest T-cell activation. Conversely, virus specific CD8+ T cells are also effective in recovery[5]. Suppression of CD8+ T cells is probably associated with the establishment of persistent infection[6,84]. Since KHF, especially KHF5, replicates faster in mouse tissues than prototype Hantaan virus strain 76–118, T-cell activation in mice are toward to increasing inflammation rather than recovery.

Although a single amino acid mutation in Gn altered the virulence of KHFV in mice, we did not determine the cause of the difference. Under KHF5 infection, viral RNA was higher in the culture supernatant, whereas viral N protein was reduced in the cells. In contrast, viral N protein showed higher induction in KHF4 inoculated cells *in vitro* and lung tissues. The results indicate that avirulent mutations may affect the release of daughter viruses. The minor difference may ultimately result in a distinct pathogenicity difference in mice. Conversely, KHF5 progeny viruses in the lungs were high under *in vivo* inoculation, but low under lung tissue inoculation, indicating that an unknown factor favors the growth of KHF5 in lung of mice.

5. Conclusions

In this study, KHF5-infected mice showed phenotypes similar to human HFRS cases, such as renal hemorrhage, pneumonia, hepatitis, and other clinicopathological changes. However, the phenotypes confirmed in this study did not include renal dysfunction. In mice, indicators besides BUN and albuminuria should also be considered. Also, inflammatory cytokines were induced but not enough to be considered as an evidence of cytokine storm in the mouse model, and the pathology progressed along with the activation of neutrophils. These observations showed the potential of KHF5-infected mice as a model for severe HFRS infection.

6. Summary

Hantaan virus is the causative agent of hemorrhagic fever with renal syndrome (HFRS). The Hantaan virus strain, Korean hemorrhagic fever virus clone-5 (KHF5), causes weight loss and renal hemorrhage in laboratory mice. Clone-4 (KHF4), which has a single E417K amino acid change in its glycoprotein is an avirulent variant. In this study, KHF4 and KHF5 were compared to evaluate pathological differences in mice *in vitro* and *in vivo*. The characteristics of the two glycoproteins were not significantly different *in vitro*. However, the virulent strain KHF5 targeted the lungs and caused pneumonia and edema *in vivo*. Both strains induced high infectivity levels in the liver and caused hepatitis; however, petechial hemorrhage and glycogen storage reduction were observed in KHF5-infected mice alone. Renal hemorrhage was observed using viral antigens in the tubular region of KHF5-infected mice. In addition, an increase in white blood cell levels and neutrophilia were found in KHF5-infected mice. Microarray analysis of liver cells showed that CD8+ T cell activation, acute-phase protein production, and neutrophil activation was induced by KHF5 infection. KHF5 infectivity was significantly increased *in vivo* and the histological and clinicopathological findings were similar to those in patients with HFRS.

Chapter 2: Serological methods for detection of infection with shrew-borne hantaviruses: Thottapalayam, Seewis, Altai, and Asama viruses

1. Introduction

Hantaviruses are enveloped single-stranded negative-sense RNA viruses that belong to the family *Hantaviridae* of the order *Bunyavirales*. Some viruses are responsible for two fatal rodent-borne zoonotic diseases in humans, HFRS and HPS. The nucleocapsid (N) protein not only plays an essential role in viral replication and assembly[56] but is also the main target for immune response and is used as a diagnostic antigen for hantavirus infection[2,14,70,84].

Various shrew-borne hantaviruses have been reported in many countries[80]. The TPMV was the first isolated hantavirus. It was isolated from *Suncus murinus* (musk shrew or Asian house shrew) captured in southern India in 1964[13]. Full-genome analysis of TPMV showed an early evolutionary divergence from rodent-borne hantaviruses[73,81], and very low or no antigenic cross-reactivity has been observed between TPMV and other rodent-borne hantaviruses[15,62]. In serological screening in Asian countries, only one human seropositive case of TPMV has been found in Thailand[61]. However, a conclusion about the infectivity and pathogenicity of TPMV to humans cannot be made because of the small number of screened cases. On the other hand, TPMV-seropositive and RNA-positive Asian house shrews have been found in Vietnam, Indonesia, India, and China[13,25,48,52,62].

Seewis orthohantavirus (SWSV) is widely distributed in European and Siberian Russia, and several species of *Sorex* shrews could be its natural hosts[49]. Ling et al. investigated a truncated SWSV N antigen since the N-terminal 120 amino acids have

been shown to be highly antigenic. They reported a low frequency of human SWSV infection and low degrees of cross-reactivity between SWSV and other types of hantaviruses. There is no evidence showing pathogenicity of SWSV to humans[49].

Phylogenetic analysis of SWSV showed well-resolved lineages organized by geographic origin[50]. Eurasian common shrews (*S. araneus*) captured in Hungary and Russia showed a highly divergent hantavirus lineage, and comparison of 300-nucleotide regions of L segments indicated that a distinct hantavirus was being maintained, and it was proved to be Altai orthohantavirus (ALTV). ALTV is distributed widely in Russia, Mongolia, and Europe and is carried by various species of shrews including *S. araneus, S. caecutiens, S. minutissimus*, and *S. roboratus* [35]. However, antigenic characterization of ALTV has not been reported yet.

Phylogenetic analysis has shown that Asama orthohantavirus (ASAV) is closer related to SWSV than to ALTV and TPMV[4]. ASAV is carried by Japanese shrew moles (*Urotrichus talpoides*) and these animals are endemic to Japan, suggesting that the distribution of ASAV is limited to Japan.

Genetic analyses indicated that shrew-borne hantaviruses are variable[3,32]. Despite numerous genetic reports, antigenic relationships among various shrew-borne viruses have not been reported because serological detection methods have been developed for only a few types of shrew-borne hantaviruses[62,70].

Recently, we reported unusually high seroprevalence among CKDu in Sri Lanka[68]. Although Sri Lankan hantavirus has not been identified yet, Thailand orthohantavirus

(THAIV)-related virus must be infected to them. THAIV is considered as not causative virus for HFRS, but significant relationship between seropositivity to THAIV and renal disease was observed in this area[68]. However, about half of CKDu patients were seronegative to THAIV. It is necessary to explore the existence of hantavirus in these areas and confirm if there is a relationship between CKDu and hantavirus infectious disease.

In this study, by using a novel serological diagnostic method, we found the first seropositive human case to ALTV antigen. Although most of the shrew-borne hantaviruses have not been isolated, the serodiagnosis method that we have developed can be used without isolated viruses. Therefore, this method is useful for further serological investigations of shrew-borne hantaviruses.

2. Materials and methods

2.1 Plasmids

The coding region of the N protein of SWSV and ALTV were amplified by PCR from shrews captured in the Khovsgol region of Mongolia, in August 2010. The PCR amplicon of SWSV was obtained from *Sorex araneus* and that of ALTV was obtained from *Sorex tundrensis*. The coding region of the N protein of ASAV (EU929070) was previously prepared[70]. The expression vector for the TPMV N protein (AY526097) with a mutation for monoclonal antibody E5/G6 binding was previously prepared[68]. Coding regions of the N proteins of SWSV, ALTV, and ASAV were insert into a

mammalian expression vector, pCAGGS/MCS[58]. Briefly, the NP coding region of SWSV, ALTV and ASAV were amplified by PCR using AmpliTaq DNA polymerase (Thermo Fisher Scientific). SWSV_NPF/ EcoRI (CACGAATTCATGGAGGATATCAAACAGTT) and SWSVNPEND-XhoI (TTTCTCGAGTCACAGCTTCATTGGCTCCA), ALTV_NPF/ EcoRI (TATGAATTCATGGCAGATATAAAGCAGGG) and ALTVNPEND-XhoI (TTTCTCGAGTTACAGCTTTAATGGTTCCT), ASAMA-16F (AGGAATTCATGGCAACATTGAGGACATCC), and ASAMA-S-1317R-XhoI (CGTCTCGAGTTACAGCTTGAGAGGATCCATGTTTGAAATC) were used as primers. The PCR products were purified by QIAquick PCR Purification Kit (Qiagen, Hilden, Germany) and digested with EcoRI (Takara, Kusatsu, Japan), XhoI (Takara), then purified by Gel purification using Wizard SV Gel and PCR Clean-up system (Promega, Madison, WI USA), according to the manufacture's direction and finally ligated with a mammalian expression plasmid vector, pCAGGS/MCS by using 2X Rapid Ligation Buffer (Promega). Finally, plasmid DNA of pCAGGS-ASAV-NP, pCAGGS-TPMV-NP, pCAGGS-ALTV-NP, and pCAGGS-SWSV-NP were prepared using Maxiprep Kit (Qiagen). Also, the coding region of N of SWSV and ALTV were inserted into the XhoI and EcoRI restriction site of expression vector pET43.1 (Novagen, Merck Millipore, Burlington MA, USA) for expression of N proteins fused with NusA and histidine-tagged protein. These constructs were designated as p43.1-ALTV-NP and p43.1-SWSV-NP.

2.2 Preparation of rabbit antisera to recombinant NP of ALTV and SWSV

The p43.1-ALTV-NP and p43.1-SWSV-NP plasmids were introduced into *E. coli* strain BL21 (DE3) and then the expression of the recombinant proteins were induced according to the manufacturer's instructions (Novagen). Recombinant N proteins were purified using HisTrap HP columns (Amersham, Piscataway, NJ, USA) according to the manufacturer's instructions. Molecular weights of purified antigens were evaluated by a Western blot assay using a mouse anti-NUS antibody (Nus•Tag™ Monoclonal Antibody, Novagen). Rabbit antisera to NUS-tagged rN of ALTV and SWSV were prepared by Sigma Aldrich Technical Service Japan.

2.3 Cells

The Vero E6 cells（ATCC C1008）were grown in MEM (MEM, Gibco, Life Technologies Corporation, NY USA) supplemented with 10% heat-inactivated fetal bovine serum (FBS, Biowest, Nuaillé), MEM Non-essential Amino Acid (Gibco), Insulin-Transferrin selenium (Gibco), penicillin (50 units/ ml), and streptomycin (50 µg/ ml) (Sigma-Aldrich Co, St Louis, MO. USA), Gentamycin (100 µg/ ml, Sigma) in a 5% CO_2 incubator at 37ºC. HEK293T cells were cultured in Dulbecco Modified Eagle Medium (DMEM, Gibco) with 10% FBS (Biowest), and 1% penicillin-streptomycin (Sigma).

2.4 Antibodies and immune sera

Rabbit antisera to TPMV-rN were prepared previously[62]. Experimentally immune mouse sera to TPMV was previously prepared[62]. Rabbit antisera to ALTV-rN and SWSV-rN were prepared as described above. Mouse monoclonal antibody E5/G6 was prepared to the N protein of Hantaan orthohantavirus[88]. The epitope sequence of E5/G6 was analyzed previously[61]. Interestingly, the N protein of ASAV had the epitope sequence for monoclonal antibody E5/G6. In previous report, rNP of TPMV having mutations to bind to E5/G6 was prepared in mammalian cells[67]. Therefore, we used E5/G6 monoclonal antibody to detect rN of TPMV and ASAV.

2.5 Transfection

HEK293T cells and Vero E6 cells (3 x 10^5 cells per 35 mm dish) were transfected with 2.5 μg plasmid DNA using 7.5 μl of LT-1 transfection reagent (Mirus, Madison, WI, USA) in 250 μl DMEM neither with serum nor antibiotics and were harvested for IFA or Western blot analysis at 48 hr after transfection.

2.6 Indirect immunofluorescence assay (IFA)

IFA tests were performed as described previously[89]. Recombinant N proteins of ASAV, TPMV, ALTV, and SWSV were expressed in Vero E6 cells and the cells were acetone-fixed on 24-well grass-slide (Matsunami, Kishiwada, Japan). Alexa Fluor 488-labeled goat anti-mouse IgG antibody (Molecular Probes, Life Technologies

Corporation, NY) was used as a secondary antibody for E5/G6 monoclonal antibody. To detect antibodies in shrew, rabbit, and human sera, Alexa Fluor 488 labeled Protein A (Molecular Probes) was used.

2.7 Western blot analysis

Proteins in the transfected HEK293T cells were separated by sodium dodecyl sultfate-polyacrylamide gel electrophoresis and transferred to a Immobilon® - P transfer membranes (Merck Millipore, Ireland). Immune rabbit sera to hantavirus rNP or monoclonal antibody E5/G6 or human sera were used as primary antibodies, and the bound antibodies were detected with HRP-conjugated protein A (Prozyme, San Leandro, CA USA) and ECL Prime Western Blotting Detection Reagent (Amersham).

2.8 Focus reduction neutralization test (FRNT)

The endpoint titers of neutralizing antibodies against TPMV were determined by FRNT as described previously[52]. Immune mouse serum was used as a positive control. Briefly, 15 µl serum was diluted in 285 µl of PBS containing 2% FBS, and then two-hold serial dilutions from 1:20 to 1:2560 were prepared. An equal volume of TPMV containing 50 focus-forming units was mixed with sera at 37℃ in a CO_2 incubator for 1h. Fifty µl of the mixture was inoculated to Vero E6 cells in a 96-well tissue-culture plate (Corning Incorporated, Costar, ME, USA). After 1h incubation at 37℃ in a CO_2 incubator, the medium was changed to 1.5% carboxymethyl cellulose contained

growth medium. After 7-day incubation in a CO_2 incubator, cells were fixed with acetone-methanol (1:1) and dried. The foci of virus-infected cells were detected by staining with rabbit antiserum to rN-TPMV as previously described [62]. The FRNT titer was expressed as the reciprocal of the highest serum dilution that resulted in more than 50% reduction in the number of infected cell foci.

2.9 Human sera

Sera from 104 renal patients collected in 2016 and 305 healthy controls collected in 2018 from Girandrukotte, Sri Lanka, were used. Sera were already examined about anti-rodent-borne hantavirus antibodies[68, 85]. Ethical approval for this study was obtained from the Institutional Ethical Review Committee, Faculty of Medicine, University of Peradeniya, Sri Lanka (2016/EC/64) and the Ethical Review Committee of the Graduate School of Medicine, Hokkaido University, Japan (M17-023).

3. Results

3.1 Expression of rNP in Vero E6 cells

To confirm the expression of rN proteins in mammalian cells, Vero E6 cells were transfected with pC-ASAV-NP, pC-TPMV-NP-Mu, pC-ALTV-NP, and pC-SWSV-NP and rN proteins were detected by an indirect immunofluorescence antibody assay (IFA) (Fig. 11B).

The rN protein of TPMV-mu that had been modified for binding with E5/G6 was used (Fig. 11A). E5/G6 showed fluorescence in the cytoplasm of pC-ASAV-NP and

pC-TPMV-mu-NP-transfected cells (Fig. 11B). Similarly, anti-rN of ALTV and SWSV immune rabbit sera showed fluorescence in cells expressing the homologous antigens. As shown in Fig. 11B, mock-transfected cells and unimmunized rabbit sera showed no specific fluorescence. These results indicated that rN proteins of ASAV, TPMV-mu, ALTV, and SWSV were successfully expressed in Vero E6 cells. Recombinant N protein of ASAV was only detected by E5/G6 and showed no-cross reactivity to antisera to TPMV-mu, ALTV, and SWSV. These results indicated highly divergent antigenic characteristics of N proteins of the four shrew-borne hantaviruses.

HEK293T cells were tranfected with plasmids pC-ASAV-NP, pC-TPMV-NP, pC-ALTV-NP, and pC-SWSV-NP. At 48 hrs after transfection, the cells were collected and lysed for Western blot assays. No cross-reactivities of immune sera among ASAV, TPMV-mu, ALTV, and SWSV were also confirmed by Western blot assays. As shown in Fig. 11C, molecular weights of detected rN proteins were around 50 kDa, which were close to the estimated sizes of N. Since degraded products were also detected, it is thought that there are sites that are easily cleaved. E5/G6 detected both rN proteins of ASAV and TPMV-mu expressed in HEK293T cells. On the other hand, anti-TPMV, ALTV, and SWSV immune sera detected only the homologous rN antigen (Fig. 11C). The use of a combination of two different assays, IFA using Vero E6 cells and Western blot assay using HEK293T cells, is expected to be effective for excluding reactivities against cellular components of Vero E6 cells observed in an IFA assay. Finally, sera

that responded to both tests, Vero E6 cell-based IFA and HEK293T-based Western blot assay, were considered as positive.

A

Virus	Site	Epitope sequence										E5/G6 -binding
Hantaan	165-174	Y	E	D	V	N	G	I	R	K	P	Yes
ASAV	166-175	Y	I	E	V	N	G	I	R	K	P	Yes
TPMV	175-185	M	E	D	R	N	G	I	K	Q	H	No
TPMV-mu	175-185	M	E	D	V	N	G	I	R	K	P	Yes
ALTV	128-137	S	E	D	A	R	G	G	R	T	P	No
SWSV	166-175	F	D	E	T	P	T	G	R	K	P	No

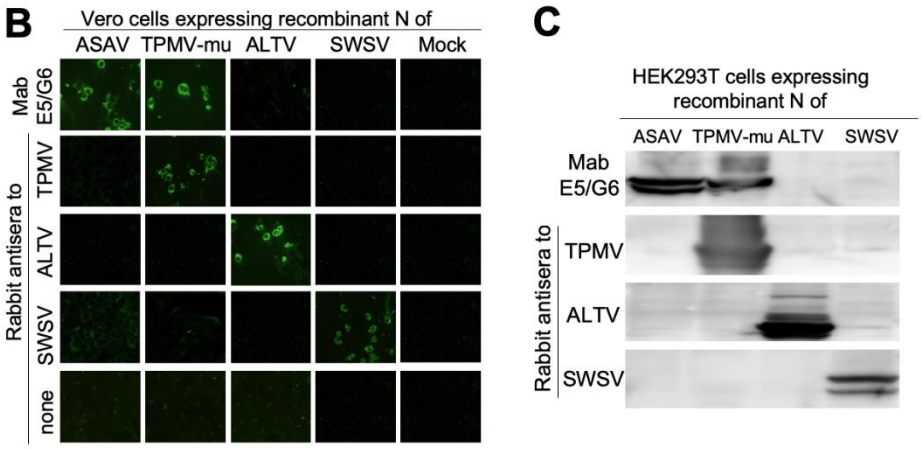

Figure 11 Expression of rN proteins of ASAV, TPMV, ALTV and SWSV.

A: Epitope sequence of E5/G6 in TPMV and ASAV. The deduced amino acid sequence of the E5/G6 epitope of ASAV is close to that of Hantaan virus. On the other hand, wild-type N of TPMV lacked binding with E5/G6. The rN of a TPMV mutant (TPMV-mu) had four amino acid substitutions to enable binding with E5/G6 [62,67]. Corresponding regions of ALTV and SWSV are also shown.

B: Vero E6 cells expressing rN on 24-well glass slides were fixed with acetone. Monoclonal antibody E5/G6 and rabbit antisera to rN of TPMV, ALTV and SWSV were used for detection of rN of ASAV, TPMV, ALTV and SWSV, respectively. Cells transfected with pCAGGS/MCS plasmid were used as negative control cells (Mock).

C: HEK293T cells transfected with rN were lysed and used as an antigen for a Western blot assay, and the same antibodies as those in B were used for detection of rN proteins.

3.2 Serological detection of shrew-borne hantavirus in human

In this study, I tried to clarify the association between shrew-borne hantavirus infection and renal diseases. Sera from 104 renal disease patients and 275 healthy controls collected from 2016 to 2018 in Girandrukotte, Sri Lanka were used[21,68]. As shown in Fig. 12A, seropositivity rates were very low and no significant difference between patients and healthy controls was found. These results indicated that there was no association between seropositivity to shrew-borne hantaviruses and renal disease. However, we found one serum specimen that was positive for ALTV antigen (#1) from patients and two serum specimens that were positive for TPMV antigen (#2 and #3) from healthy controls. Western blot profiles of these sera are shown in Fig. 12B. In IFA, serum specimen #1, #2 and #3 also showed specific reactions to ALTV and TPMV (data not shown). Interestingly, specimens #1 and #3 were also THAIV-seropositive in previous studies[68,89]. Because of the lack of antigenic cross-reactivities of N antigen among TPMV, ALTV, and THAIV, transmission of TPMV or ALTV from shrews and transmission of THAIV from rodents might have occurred independently in this area. For further antigenic comparison, focus reduction neutralization (FRNT) assays were carried out as previously described[52]. Although the anti-TPMV immune serum used as a positive control showed a high FRNT titer of over 160[62], neither #2 nor #3 showed a significant focus reduction (<20). These results suggested that a TPMV-related but serologically distinct virus might have infected

humans in Girandurukotte, Sri Lanka. Unfortunately, isolated ALTV was not available, and we could not perform an FRNT assay for ALTV.

A

	Tested	ASAV	TPMV	ALTV	SWSV	THAIV
Renal Patients	104	0	0	1 (#1)	0	61
Healthy control	271	0	2 (#2, 3)	0	0	52

B

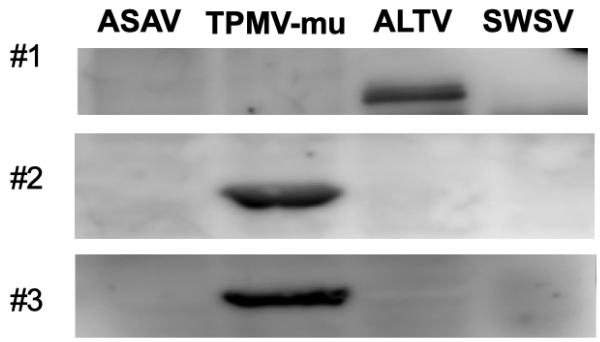

Figure 12 Serological screening of human sera by using rN of ASAV, TPMV-mu, ALTV, and SWSV.

A: Numbers sera that are positive to ASAV, TPMV-mu, ALTV, and SWSV were confirmed by two tests, IFA and Western blot assay, at a serum dilution of 1:100. Number of antibody positives to THAIV was confirmed by two IFA tests by using rN of THAIV-expressing cells and THAIV-infected cells as previously described[69]. We found one seropositive for ALTV antigen (#1) from renal diseases patients and two seropositives for TPMV-mu antigen (#2 and #3) from healthy controls.

B: Western blot patterns of human sera #1, 2, and 3 to rN antigens of ASAV, TPMV, ALTV, and SWSV.

4. Discussion

In this study, rN antigens of four shrew-borne viruses, TPMV, ASAV, ALTV, and SWSV were produced. Recombinant antigens expressed in two different mammalian cells, Vero E6 cells and 293T cells, were useful as IFA and Western blot antigen, respectively.

Various shrew-borne hantaviruses were reported from many countries. Genetic analyses indicated that the shrew-borne hantaviruses are more variable than rodent-borne hantaviruses[3]. It is believed that rodent-borne viruses were offspring of host-switched virus from shrew-borne hantaviruses[32]. In spite of numerous genetic reports, antigenic relationship among various shrew-borne viruses were not reported. Also, the serological detection methods have been developed for a few types of shrew-borne hantaviruses.

SWSV is widely distributed, and its reservoir was not unique. Several species of *Sorex* shrews could be its natural hosts. Ling et al expressed the recombinant N antigen of SWSV for production of antisera and they showed no cross-reactivity to rodent-borne hantaviruses[50]. Next, they expressed the entire N protein of Finish SWSV as IFA and Western blot antigens[49]. They found cross-reactivity of rabbit anti-rN antiserum of SWSV to Puumala virus. On the other hand, most of Puumala virus-positive human sera were negative to the SWSV antigen except several sera. They

concluded that several positives were considered to be due to cross-reactivity to Puumala antigen. Indeed, no case by SWSV infection was reported. These observations indicated low frequency of human SWSV infection and low cross-reactivity between SWSV and other hantaviruses.

TPMV is considered to be distributed to Asian countries according to the distribution of *S. murinus*. Because TPMV was isolated and adapted to cell culture, focus-reduction neutralization assay is available. It is well known that TPMV has distinct antigenicity from other hantaviruses. Okumura et al. reported that antigenicity of the N protein of TPMV was not cross-reactive except a part of the Gc region which is the common antigenic site of hantaviruses[62]. Using monoclonal antibodies Schlegel et al. also showed that antigenicity of TPMV NP was unique and no cross-reactive antigenicity was found between TPMV and ASAV[70]. Throughout serological screening in Asian countries, only one human seropositive case was found in Thailand [52,62]. However, the infectivity and pathogenicity of TPMV to humans have not conclusively proven because of low number of screened cases. On the other hand, seropositive and TPMV genome-positive animals were found in Viet Nam, Indonesia, India, and China.

ALTV is a sorex-borne hantavirus but belongs to distinct lineage from SWSV. ALTV distributes widely in Russia, Mongolia, and Europe, carried by various shrews

such as *S. araneus*, *S. caecutiens*, *S. minutissimus*, and *S. roboratus*[35]. However, antigenic characterization of ALTV has not been reported yet.

ASAV is relatively closed to SWSV rather than ALTV and TPMV in phylogenetic analysis[4]. ASAV is carried by Japanese shrew mole (*Urotrichus talpoides*) and this animal is endemic to Japan, suggesting that distribution of ASAV is limited in Japan.

In this study, we tried to screen the patients and control sera by using shrew-borne hantavirus antigens distinct from THAIV. The TPMV seropositive sera without FRNT activities were detected from a healthy control. Although I also found a seropositive serum to the ALTV antigen from the CKDu patient group, no significant relationship between seropositivity and renal disease was found. A total 3 of 375 samples showed shrew-borne hantavirus-seropositive, suggested the potential infectivity of shrew-borne hantaviruses to humans. However, there is still no strong evidence showing that these viruses caused renal disease in humans. In Sri Lanka, TPMV or ALTV- positive shrews have not been reported yet. However, Sri Lanka is a habitat of many species of shrews. It is necessary to find shrews species carrying hantaviruses in the country. Recently, Qi et al. suggested that the N protein of Imjin virus shows no antigenic cross-reactivities to rodent-borne hantavirus, and they also suggested Imjin or Imjin-like virus infection in humans in China[64]. Their results also suggested that potential human infection of shrew-borne virus has occurred in various countries.

5. Summary

The infectivity of shrew-borne hantaviruses to humans is still unclear because of the lack of a serodiagnosis method for these viruses. In this study, we prepared rN proteins of ASAV, TPMV, ALTV, and SWSV. Using monospecific rabbit sera, no antigenic cross-reactivities were observed among these viruses. In a serosurvey of 104 samples from renal patients and 271 samples from heathy controls from Sri Lanka, one patient and two healthy control sera reacted with rN proteins of ALTV and TPMV, respectively. The novel assays should be applied to investigate potential infection of humans with shrew-borne hantaviruses.

Conclusions

BALB/c mice infected with the HTNV strain KHF5 were used to analyze hantavirus pathogenesis. KHFV targeted lungs and caused immunopathogenesis in the lungs and liver with neutrophilia, monocyte infiltration, and CD8+ T cell activation, followed by pneumonia, edema, hepatitis, and renal tubular hemorrhage with proteinuria. The *in vivo* factors that dramatically increased KHF5 infectivity remain unclear. In the future, more evidence will be needed to prove kidney dysfunction and cytokine storms, which are generally involved in hantavirus pathogenesis.

The antigenic diversity of four shrew-borne hantavirus antigens, ASAV, TPMV, ALTV, and SWSV N proteins were confirmed by IFA and western blot, and novel serological diagnostic methods using N antigens were established. Then, sera from 104 renal disease patients and 271 healthy controls from Sri Lanka were screened. One serum sample from a patient with CKDu tested positive for ALTV and two healthy control sera were positive for TPMV. These results show the infectivity of ALTV and TPMV to humans, but evidence to show shrew-borne hantavirus pathogenicity, which may cause renal disease, is still lacking.

Although HFRS is thought to be caused by rodent-borne hantaviruses, the results of this study suggest a need to pay more attention to shrew and bat-borne hantaviruses with unknown infectivity to humans. The novel serological diagnostic method established in this study provides researchers with a fast and accurate tool to study

shrew-borne hantavirus epidemiology. Through epidemiological studies, we can learn how anthropological environmental changes affect animal movements, who can potentially carry zoonotic viruses. This study will assist researchers in identifying these animals, locating them, and identifying those that carry viruses that pose a risk to public health. Furthermore, the pathological aspects revealed in this study could help to develop treatments for infectious diseases. Overall, this study promotes a further step towards the goal of One-Health.

Reference

1. Alexeyev, O. A., Elgh, F., Zhestkov, A. V., Wadell, G., and Juto, P. 1996. Hantaan and Puumala virus antibodies in blood donors in Samara, an HFRS-endemic region in European Russia. *Lancet* **347**, 1483
2. Amada, T., Yoshimatsu, K., Yasuda, S. P., Shimizu, K., Koma, T., Hayashimoto, N., Gamage, C. D., Nishio, S., Takakura, A., and Arikawa, J. 2013. Rapid, whole blood diagnostic test for detecting anti-hantavirus antibody in rats. *J Virol Methods* **193**, 42-49
3. Arai, S., Bennett, S. N., Sumibcay, L., Cook, J. A., Song, J. W., Hope, A., Parmenter, C., Nerurkar, V. R., Yates, T. L., and Yanagihara, R. 2008. Phylogenetically distinct hantaviruses in the masked shrew (*Sorex cinereus*) and dusky shrew (*Sorex monticolus*) in the United States. *Am J Trop Med Hyg* **78**, 348-351
4. Arai, S., Ohdachi, S. D., Asakawa, M., Kang, H. J., Mocz, G., Arikawa, J., Okabe, N., and Yanagihara, R. 2008. Molecular phylogeny of a newfound hantavirus in the Japanese shrew mole (*Urotrichus talpoides*). *Proc Natl Acad Sci U S A* **105**, 16296-16301
5. Araki, K., Yoshimatsu, K., Lee, B. H., Kariwa, H., Takashima, I., and Arikawa, J. 2003. Hantavirus-specific CD8(+)-T-cell responses in newborn mice persistently infected with Hantaan virus. *J Virol* **77**, 8408-8417
6. Araki, K., Yoshimatsu, K., Lee, B. H., Kariwa, H., Takashima, I., and Arikawa, J. 2004. A new model of Hantaan virus persistence in mice: the balance between HTNV infection and CD8(+) T-cell responses. *Virology* **322**, 318-327
7. Arikawa, J., Schmaljohn, A. L., Dalrymple, J. M., and Schmaljohn, C. S. 1989. Characterization of Hantaan virus envelope glycoprotein antigenic determinants defined by monoclonal antibodies. *J Gen Virol* **70**, 615-624

8. Arikawa, J., Takashima, I., and Hashimoto, N. 1985. Cell fusion by haemorrhagic fever with renal syndrome (HFRS) viruses and its application for titration of virus infectivity and neutralizing antibody. *Arch Virol* **86**, 303-313

9. Asada, H., Balachandra, K., Tamura, M., Kondo, K., and Yamanishi, K. 1989. Cross-reactive immunity among different serotypes of virus causing haemorrhagic fever with renal syndrome. *J Gen Virol* **70 (Pt 4)**, 819-825

10. Athuraliya, N. T., Abeysekera, T. D., Amerasinghe, P. H., Kumarasiri, R., Bandara, P., Karunaratne, U., Milton, A. H., and Jones, A. L. 2011. Uncertain etiologies of proteinuric-chronic kidney disease in rural Sri Lanka. *Kidney Int* **80**, 1212-1221

11. Avsic-Zupanc, T., Poljak, M., Furlan, P., Kaps, R., Xiao, S. Y., and Leduc, J. W. 1994. Isolation of a strain of a Hantaan virus from a fatal case of hemorrhagic fever with renal syndrome in Slovenia. *Am J Trop Med Hyg* **51**, 393-400

12. Brummer-Korvenkontio, M., Vaheri, A., Hovi, T., von Bonsdorff, C. H., Vuorimies, J., Manni, T., Penttinen, K., Oker-Blom, N., and Lahdevirta, J. 1980. Nephropathia epidemica: detection of antigen in bank voles and serologic diagnosis of human infection. *J Infect Dis* **141**, 131-134

13. Carey, D. E., Reuben, R., Panicker, K. N., Shope, R. E., and Myers, R. M. 1971. Thottapalayam virus: a presumptive arbovirus isolated from a shrew in India. *Indian J Med Res* **59**, 1758-1760

14. Cautivo, K., Schountz, T., Acuña-Retamar, M., Ferrés, M., and Torres-Pérez, F. 2014. Rapid enzyme-linked immunosorbent assay for the detection of hantavirus-specific antibodies in divergent small mammals. *Viruses* **6**, 2028-2037

15. Chu, Y. K., Jennings, G., Schmaljohn, A., Elgh, F., Hjelle, B., Lee, H. W., Jenison, S., Ksiazek, T., Peters, C. J., and Rollin, P. 1995. Cross-neutralization

of hantaviruses with immune sera from experimentally infected animals and from hemorrhagic fever with renal syndrome and hantavirus pulmonary syndrome patients. *J Infect Dis* **172**, 1581-1584

16. Clement, J., Maes, P., and Van Ranst, M. 2014. Hemorrhagic fever with renal syndrome in the New, and hantavirus pulmonary syndrome in the Old World: paradi(se)gm lost or regained? *Virus Res* **187**, 55-58
17. Duchin, J. S., Koster, F. T., Peters, C. J., Simpson, G. L., Tempest, B., Zaki, S. R., Ksiazek, T. G., Rollin, P. E., Nichol, S., and Umland, E. T. 1994. Hantavirus pulmonary syndrome: a clinical description of 17 patients with a newly recognized disease. The hantavirus study group. *N Engl J Med* **330**, 949-955
18. Ettinger, J., Hofmann, J., Enders, M., Tewald, F., Oehme, R. M., Rosenfeld, U. M., Ali, H. S., Schlegel, M., Essbauer, S., Osterberg, A., Jacob, J., Reil, D., Klempa, B., Ulrich, R. G., and Kruger, D. H. 2012. Multiple synchronous outbreaks of Puumala virus, Germany, 2010. *Emerg Infect Dis* **18**, 1461-1464
19. Faber, M. S., Ulrich, R. G., Frank, C., Brockmann, S. O., Pfaff, G. M., Jacob, J., Krüger, D. H., and Stark, K. 2010. Steep rise in notified hantavirus infections in Germany, April 2010. *Euro Surveill* **15** (20), 19574
20. Gajdusek, D. C. 1962. Virus hemorrhagic fevers. Special reference to hemorrhagic fever with renal syndrome (epidemic hemorrhagic fever). *J Pediatr* **60**, 841-857
21. Gamage, C. D., Yoshimatsu, K., Sarathkumara, Y. D., Kulendiran, T., Nanayakkara, N., and Arikawa, J. 2017. Serological evidence of hantavirus infection in Girandurukotte, an area endemic for chronic kidney disease of unknown aetiology (CKDu) in Sri Lanka. *Int J Infect Dis* **57**, 77-78
22. Garanina, E., Martynova, E., Davidyuk, Y., Kabwe, E., Ivanov, K., Titova, A., Markelova, M., Zhuravleva, M., Cherepnev, G., Shakirova, V. G., Khaertynova, I., Tarlinton, R., Rizvanov, A., Khaiboullina, S., and Morzunov,

S. 2019. Cytokine storm combined with humoral immune response defect in fatal hemorrhagic fever with renal syndrome case, Tatarstan, Russia. *Viruses* **11** (7), 601

23. Gnemmi, V., Verine, J., Vrigneaud, L., Glowacki, F., Ratsimbazafy, A., Copin, M. C., Dewilde, A., and Buob, D. 2015. Microvascular inflammation and acute tubular necrosis are major histologic features of hantavirus nephropathy. *Hum Pathol* **46**, 827-835

24. Gorbunova, E., Gavrilovskaya, I. N., and Mackow, E. R. 2010. Pathogenic hantaviruses Andes virus and Hantaan virus induce adherens junction disassembly by directing vascular endothelial cadherin internalization in human endothelial cells. *J Virol* **84**, 7405-7411

25. Guo, W. P., Lin, X. D., Wang, W., Zhang, X. H., Chen, Y., Cao, J. H., Ni, Q. X., Li, W. C., Li, M. H., Plyusnin, A., and Zhang, Y. Z. 2011. A new subtype of Thottapalayam virus carried by the Asian house shrew (*Suncus murinus*) in China. *Infect Genet Evol* **11**, 1862-1867

26. Han, W. K., Bailly, V., Abichandani, R., Thadhani, R., and Bonventre, J. V. 2002. Kidney injury molecule-1 (KIM-1): a novel biomarker for human renal proximal tubule injury. *Kidney Int* **62**, 237-244

27. He, W., Fu, J., Wen, Y., Cheng, M., Mo, Y., and Chen, Q. 2021. Detection and genetic characterization of seoul virus in liver tissue samples from *Rattus norvegicus* and *Rattus tanezumi* in Urban Areas of Southern China. *Front Vet Sci* **8**, 748232

28. Hofmann, J., Meisel, H., Klempa, B., Vesenbeckh, S. M., Beck, R., Michel, D., Schmidt-Chanasit, J., Ulrich, R. G., Grund, S., Enders, G., and Kruger, D. H. 2008. Hantavirus outbreak, Germany, 2007. *Emerg Infect Dis* **14**, 850-852

29. Hooper, J., Paolino, K. M., Mills, K., Kwilas, S., Josleyn, M., Cohen, M., Somerville, B., Wisniewski, M., Norris, S., Hill, B., Sanchez-Lockhart, M., Hannaman, D., and Schmaljohn, C. S. 2020. A phase 2a randomized, double-

blind, dose-optimizing study to evaluate the immunogenicity and safety of a bivalent DNA vaccine for hemorrhagic fever with renal syndrome delivered by intramuscular electroporation. *Vaccines (Basel)* **8** (3), 377

30. ICTV Viruses taxonomy: 2021 release. Available online: https:// talk.ictvonline.org/taxonomy/ (accessed on 14 September 2022).

31. Jangra, R. K., Herbert, A. S., Li, R., Jae, L. T., Kleinfelter, L. M., Slough, M. M., Barker, S. L., Guardado-Calvo, P., Roman-Sosa, G., Dieterle, M. E., Kuehne, A. I., Muena, N. A., Wirchnianski, A. S., Nyakatura, E. K., Fels, J. M., Ng, M., Mittler, E., Pan, J., Bharrhan, S., Wec, A. Z., Lai, J. R., Sidhu, S. S., Tischler, N. D., Rey, F. A., Moffat, J., Brummelkamp, T. R., Wang, Z., Dye, J. M., and Chandran, K. 2018. Protocadherin-1 is essential for cell entry by New World hantaviruses. *Nature* **563**, 559-563

32. Johansson, P., Yap, G., Low, H. T., Siew, C. C., Kek, R., Ng, L. C., and Bucht, G. 2010. Molecular characterization of two hantavirus strains from different rattus species in Singapore. *Virol J* **7**, 15

33. Jonsson, C. B., Figueiredo, L. T., and Vapalahti, O. 2010. A global perspective on hantavirus ecology, epidemiology, and disease. *Clin Microbiol Rev* **23**, 412-441

34. Jung, J., Ko, S. J., Oh, H. S., Moon, S. M., Song, J. W., and Huh, K. 2018. Protective effectiveness of inactivated hantavirus vaccine against hemorrhagic fever with renal syndrome. *J Infect Dis* **217**, 1417-1420

35. Kang, H. J., Gu, S. H., Yashina, L. N., Cook, J. A., and Yanagihara, R. 2019. Highly divergent genetic variants of soricid-borne Altai virus (hantaviridae) in Eurasia suggest ancient jost-switching events. *Viruses* **11** (9), 857

36. Khaiboullina, S. F., Levis, S., Morzunov, S. P., Martynova, E. V., Anokhin, V. A., Gusev, O. A., St Jeor, S. C., Lombardi, V. C., and Rizvanov, A. A. 2017. Serum cytokine profiles differentiating hemorrhagic fever with renal syndrome and hantavirus pulmonary syndrome. *Front Immunol* **8**, 567

37. Kim, H. K., Chung, J. H., Kim, D. M., Yun, N. R., Kim, C. M., and Jalal, S. 2019. Hemorrhagic fever with renal syndrome as a cause of acute diarrhea. *Am J Trop Med Hyg* **100**, 1236-1239

38. Kim, W. K., Kim, J. A., Song, D. H., Lee, D., Kim, Y. C., Lee, S. Y., Lee, S. H., No, J. S., Kim, J. H., Kho, J. H., Gu, S. H., Jeong, S. T., Wiley, M., Kim, H. C., Klein, T. A., Palacios, G., and Song, J. W. 2016. Phylogeographic analysis of hemorrhagic fever with renal syndrome patients using multiplex PCR-based next generation sequencing. *Sci Rep* **6**, 26017

39. Koma, T., Yoshimatsu, K., Nagata, N., Sato, Y., Shimizu, K., Yasuda, S. P., Amada, T., Nishio, S., Hasegawa, H., and Arikawa, J. 2014. Neutrophil depletion suppresses pulmonary vascular hyperpermeability and occurrence of pulmonary edema caused by hantavirus infection in C.B-17 SCID mice. *J Virol* **88**, 7178-7188

40. Krakauer, T., Leduc, J. W., and Krakauer, H. 1995. Serum levels of tumor necrosis factor-alpha, interleukin-1, and interleukin-6 in hemorrhagic fever with renal syndrome. *Viral Immunol* **8**, 75-79

41. Krautkramer, E., Nusshag, C., Baumann, A., Schafer, J., Hofmann, J., Schnitzler, P., Klempa, B., Witkowski, P. T., Kruger, D. H., and Zeier, M. 2016. Clinical characterization of two severe cases of hemorrhagic fever with renal syndrome (HFRS) caused by hantaviruses Puumala and Dobrava-Belgrade genotype Sochi. *BMC Infect Dis* **16**, 675

42. Krüger, D. H., Schönrich, G., and Klempa, B. 2011. Human pathogenic hantaviruses and prevention of infection. *Hum Vaccin* **7**, 685-693

43. Latronico, F., Maki, S., Rissanen, H., Ollgren, J., Lyytikainen, O., Vapalahti, O., and Sane, J. 2018. Population-based seroprevalence of Puumala hantavirus in Finland: smoking as a risk factor. *Epidemiol Infect* **146**, 367-371

44. Lee, D. W., Gardner, R., Porter, D. L., Louis, C. U., Ahmed, N., Jensen, M., Grupp, S. A., and Mackall, C. L. 2014. Current concepts in the diagnosis and management of cytokine release syndrome. *Blood* **124**, 188-195

45. Lee, H. W., Baek, L. J., and Johnson, K. M. 1982. Isolation of Hantaan virus, the etiologic agent of Korean hemorrhagic fever, from wild urban rats. *J Infect Dis* **146**, 638-644

46. Lee, H. W., and Cho, H. J. 1981. Electron microscope appearance of Hantaan virus, the causative agent of Korean haemorrhagic fever. *Lancet* **1**, 1070-1072

47. Lee, H. W., Lee, P. W., and Johnson, K. M. 1978. Isolation of the etiologic agent of Korean hemorrhagic fever. *J Infect Dis* **137**, 298-308

48. Lin, X. D., Zhou, R. H., Fan, F. N., Ying, X. H., Sun, X. Y., Wang, W., Holmes, E. C., and Zhang, Y. Z. 2014. Biodiversity and evolution of Imjin virus and Thottapalayam virus in *Crocidurinae* shrews in Zhejiang Province, China. *Virus Res* **189**, 114-120

49. Ling, J., Sironen, T., Voutilainen, L., Hepojoki, S., Niemimaa, J., Isoviita, V. M., Vaheri, A., Henttonen, H., and Vapalahti, O. 2014. Hantaviruses in Finnish soricomorphs: evidence for two distinct hantaviruses carried by *Sorex araneus* suggesting ancient host-switch. *Infect Genet Evol* **27**, 51-61

50. Ling, J., Smura, T., Tamarit, D., Huitu, O., Voutilainen, L., Henttonen, H., Vaheri, A., Vapalahti, O., and Sironen, T. 2018. Evolution and postglacial colonization of Seewis hantavirus with *Sorex araneus* in Finland. *Infect Genet Evol* **57**, 88-97

51. Liu, R., Ma, H., Shu, J., Zhang, Q., Han, M., Liu, Z., Jin, X., Zhang, F., and Wu, X. 2019. Vaccines and therapeutics against hantaviruses. *Front Microbiol* **10**, 2989

52. Luan, V. D., Yoshimatsu, K., Endo, R., Taruishi, M., Huong, V. T., Dat, D. T., Tien, P. C., Shimizu, K., Koma, T., Yasuda, S. P., Nhi, L., and Arikawa, J.

2012. Studies on hantavirus infection in small mammals captured in southern and central highland area of Vietnam. *J Vet Med Sci* **74**, 1155-1162

53. Ma, R., Zhang, X., Shu, J., Liu, Z., Sun, W., Hou, S., Lv, Y., Ying, Q., Wang, F., Jin, X., Liu, R., and Wu, X. 2021. *Nlrc3* knockout mice showed renal pathological changes after HTNV infection. *Front Immunol* **12**, 692509

54. Maas, M., van Heteren, M., de Vries, A., Kuiken, T., Hoornweg, T., Veldhuis Kroeze, E., and Rockx, B. 2019. Seoul virus tropism and pathology in naturally infected feeder rats. *Viruses* **11** (6), 531

55. Mustonen, J., Vapalahti, O., Henttonen, H., Pasternack, A., and Vaheri, A. 1998. Epidemiology of hantavirus infections in Europe. *Nephrol Dial Transplant* **13**, 2729-2731

56. Muyangwa, M., Martynova, E. V., Khaiboullina, S. F., Morzunov, S. P., and Rizvanov, A. A. 2015. Hantaviral proteins: structure, functions, and role in hantavirus infection. *Front Microbiol* **6**, 1326

57. Nichol, S. T., Spiropoulou, C. F., Morzunov, S., Rollin, P. E., Ksiazek, T. G., Feldmann, H., Sanchez, A., Childs, J., Zaki, S., and Peters, C. J. 1993. Genetic identification of a hantavirus associated with an outbreak of acute respiratory illness. *Science* **262**, 914-917

58. Niwa, H., Yamamura, K., and Miyazaki, J. 1991. Efficient selection for high-expression transfectants with a novel eukaryotic vector. *Gene* **108**, 193-199

59. Noack, D., Goeijenbier, M., Reusken, C., Koopmans, M. P. G., and Rockx, B. H. G. 2020. Orthohantavirus pathogenesis and cell tropism. *Front Cell Infect Microbiol* **10**, 399

60. Ogino, M., Ebihara, H., Lee, B. H., Araki, K., Lundkvist, A., Kawaoka, Y., Yoshimatsu, K., and Arikawa, J. 2003. Use of vesicular stomatitis virus pseudotypes bearing Hantaan or Seoul virus envelope proteins in a rapid and safe neutralization test. *Clin Diagn Lab Immunol* **10**, 154-160

61. Okumura, M., Yoshimatsu, K., Araki, K., Lee, B. H., Asano, A., Agui, T., and Arikawa, J. 2004. Epitope analysis of monoclonal antibody E5/G6, which binds to a linear epitope in the nucleocapsid protein of hantaviruses. *Arch Virol* **149**, 2427-2434

62. Okumura, M., Yoshimatsu, K., Kumperasart, S., Nakamura, I., Ogino, M., Taruishi, M., Sungdee, A., Pattamadilok, S., Ibrahim, I. N., Erlina, S., Agui, T., Yanagihara, R., and Arikawa, J. 2007. Development of serological assays for Thottapalayam virus, an insectivore-borne hantavirus. *Clin Vaccine Immunol* **14**, 173-181

63. Pattamadilok, S., Lee, B. H., Kumperasart, S., Yoshimatsu, K., Okumura, M., Nakamura, I., Araki, K., Khoprasert, Y., Dangsupa, P., Panlar, P., Jandrig, B., Kruger, D. H., Klempa, B., Jakel, T., Schmidt, J., Ulrich, R., Kariwa, H., and Arikawa, J. 2006. Geographical distribution of hantaviruses in Thailand and potential human health significance of Thailand virus. *Am J Trop Med Hyg* **75**, 994-1002

64. Qi, R., Sun, X. F., Qin, X. R., Wang, L. J., Zhao, M., Jiang, F., Wang, L., Lei, X. Y., Liu, J. W., and Yu, X. J. 2019. Suggestive serological evidence of infection with shrew-borne Imjin virus (*Viruses* **11** (12), 1128

65. Rajapakse, S., Shivanthan, M. C., and Selvarajah, M. 2016. Chronic kidney disease of unknown etiology in Sri Lanka. *Int J Occup Environ Health* **22**, 259-2640

66. Rupasinghe, S., Bowattage, S., Herath, L., and Rajaratnam, A. 2021. Two Atypical cases of hantavirus infection: experience from a tertiary care unit in Sri Lanka. *Case Rep Infect Dis* **2021**, 5555613

67. Saasa, N., Yoshida, H., Shimizu, K., Sanchez-Hernandez, C., Romero-Almaraz Mde, L., Koma, T., Sanada, T., Seto, T., Yoshii, K., Ramos, C., Yoshimatsu, K., Arikawa, J., Takashima, I., and Kariwa, H. 2012. The N-terminus of the Montano virus nucleocapsid protein possesses broadly cross-

reactive conformation-dependent epitopes conserved in rodent-borne hantaviruses. *Virology* **428**, 48-57

68. Sarathkumara, Y. D., Gamage, C. D., Lokupathirage, S., Muthusinghe, D. S., Nanayakkara, N., Gunarathne, L., Shimizu, K., Tsuda, Y., Arikawa, J., and Yoshimatsu, K. 2019. Exposure to hantavirus is a risk factor associated with kidney diseases in Sri Lanka: A cross sectional study. *Viruses* **11** (8), 700

69. Schindelin, J., Arganda-Carreras, I., Frise, E. Kaynig,V., Longair,M., Pietzsch,T., Preibisch,S, Rueden,C., Saalfeld,S., Schmid,B., Tinevez,J.Y., James White,D., Hartenstein,V., Eliceiri,K., Tomancak, P., and Cardona, A. 2012. Fiji: An open-source platform for biological-image analysis. Nat Methods **9**, 676–682

70. Schlegel, M., Tegshduuren, E., Yoshimatsu, K., Petraityte, R., Sasnauskas, K., Hammerschmidt, B., Friedrich, R., Mertens, M., Groschup, M. H., Arai, S., Endo, R., Shimizu, K., Koma, T., Yasuda, S., Ishihara, C., Ulrich, R. G., Arikawa, J., and Köllner, B. 2012. Novel serological tools for detection of Thottapalayam virus, a Soricomorpha-borne hantavirus. *Arch Virol* **157**, 2179-2187

71. Shimizu, K., Koma, T., Yoshimatsu, K., Tsuda, Y., Isegawa, Y., and Arikawa, J. 2017. Appearance of renal hemorrhage in adult mice after inoculation of patient-derived hantavirus. *Virol J* **14** (1), 13

72. Shimizu, K., Yoshimatsu, K., Taruishi, M., Tsuda, Y., and Arikawa, J. 2018. Involvement of CD8(+) T cells in the development of renal hemorrhage in a mouse model of hemorrhagic fever with renal syndrome. *Arch Virol* **163**, 1577-1584

73. Song, J. W., Kang, H. J., Gu, S. H., Moon, S. S., Bennett, S. N., Song, K. J., Baek, L. J., Kim, H. C., O'Guinn, M. L., Chong, S. T., Klein, T. A., and Yanagihara, R. 2009. Characterization of Imjin virus, a newly isolated

hantavirus from the Ussuri white-toothed shrew (*Crocidura lasiura*). *J Virol* **83**, 6184-6191

74. Strandin, T., Makela, S., Mustonen, J., and Vaheri, A. 2018. Neutrophil activation in acute hemorrhagic fever with renal syndrome is mediated by hantavirus-infected microvascular endothelial Cells. *Front Immunol* **9**, 2098

75. Tamura, M., Asada, H., Kondo, K., Tanishita, O., Kurata, T., and Yamanishi, K. 1989. Pathogenesis of Hantaan virus in mice. *J Gen Virol* **70** (Pt 11), 2897-2906

76. Tariq, M., and Kim, D. M. 2022. Hemorrhagic fever with renal syndrome: literature review, epidemiology, clinical picture and pathogenesis. *Infect Chemother* **54**, 1-19

77. Taylor, S. L., Wahl-Jensen, V., Copeland, A. M., Jahrling, P. B., and Schmaljohn, C. S. 2013. Endothelial cell permeability during hantavirus infection involves factor XII-dependent increased activation of the kallikrein-kinin system. *PLoS Pathog* **9** (7), e1003470

78. Vaheri, A., Strandin, T., Jaaskelainen, A. J., Vapalahti, O., Jarva, H., Lokki, M. L., Antonen, J., Leppanen, I., Makela, S., Meri, S., and Mustonen, J. 2014. Pathophysiology of a severe case of Puumala hantavirus infection successfully treated with bradykinin receptor antagonist icatibant. *Antiviral Res* **111**, 23-25

79. van Leeuwen, L. P. M., de Jong, W., Doornekamp, L., van Gorp, E. C. M., Wismans, P. J., and Goeijenbier, M. 2022. Exotic viral hepatitis: A review on epidemiology, pathogenesis, and treatment. *J Hepatol* 77(5):1431-1443

80. Xu, M. J., Feng, D., Wu, H., Wang, H., Chan, Y., Kolls, J., Borregaard, N., Porse, B., Berger, T., Mak, T. W., Cowland, J. B., Kong, X., and Gao, B. 2015. Liver is the major source of elevated serum lipocalin-2 levels after bacterial infection or partial hepatectomy: a critical role for IL-6/STAT3. *Hepatology* **61**, 692-702

81. Yadav, P. D., Vincent, M. J., and Nichol, S. T. 2007. Thottapalayam virus is genetically distant to the rodent-borne hantaviruses, consistent with its isolation from the Asian house shrew (*Suncus murinus*). *Virol J* **4**, 80

82. Yanagihara, R., Gu, S. H., Arai, S., Kang, H. J., and Song, J. W. 2014. Hantaviruses: rediscovery and new beginnings. *Virus Res* **187**, 6-14

83. Yao, J. S., Kariwa, H., Takashima, I., Yoshimatsu, K., Arikawa, J., and Hashimoto, N. 1992. Antibody-dependent enhancement of hantavirus infection in macrophage cell lines. *Arch Virol* **122**, 107-118

84. Yasuda, S. P., Shimizu, K., Koma, T., Hoa, N. T., Le, M. Q., Wei, Z., Muthusinghe, D. S., Lokupathirage, S. M. W., Hasebe, F., Yamashiro, T., Arikawa, J., and Yoshimatsu, K. 2021. Immunological responses to Seoul orthohantavirus in experimentally and naturally infected brown rats (*Rattus norvegicus*). *Viruses* **13** (4), 665

85. Yoshimatsu, K., Arai, S., Shimizu, K., Tsuda, Y., Boldgiv, B., Boldbaatar, B., Sergelen, E., Ariunzaya, D., Enkhmanda, O., Tuvshintugs, S., Morikawa, S., and Arikawa, J. 2017. Antibody detection from Middendorf's vole (*Microtus middendorffii*) against Tula virus captured in Mongolia. *Jpn J Vet Res* **65**, 39-44

86. Yoshimatsu, K., and Arikawa, J. 2014. Serological diagnosis with recombinant N antigen for hantavirus infection. *Virus Res* **187**, 77-83

87. Yoshimatsu, K., Arikawa, J., Ohbora, S., and Itakura, C. 1997. Hantavirus infection in SCID mice. *J Vet Med Sci* **59** (10), 863-868

88. Yoshimatsu, K., Arikawa, J., Tamura, M., Yoshida, R., Lundkvist, A., Niklasson, B., Kariwa, H., and Azuma, I. 1996. Characterization of the nucleocapsid protein of Hantaan virus strain 76-118 using monoclonal antibodies. *J gen Virol* **77**, 695-704

89. Yoshimatsu, K., Gamage, C. D., Sarathkumara, Y. D., Kulendiran, T., Muthusinghe, D. S., Nanayakkara, N., Gunarathne, L., Shimizu, K., Tsuda, Y.,

and Arikawa, J. 2019. Thailand orthohantavirus infection in patients with chronic kidney disease of unknown aetiology in Sri Lanka. *Arch Virol* **164**, 267-271

90. Young, J. C., Mills, J. N., Enria, D. A., Dolan, N. E., Khan, A. S., and Ksiazek, T. G. 1998. New World hantaviruses. *Br Med Bull* **54**, 659-673

91. Zhang, Y. Z., Lin, X. D., Shi, N. F., Wang, W., Liao, X. W., Guo, W. P., Fan, F. N., Huang, X. M., Li, M. H., Li, M. F., Chen, Y., Chen, X. P., Wang, S. B., Fu, Z. F., and Plyusnin, A. 2010. Hantaviruses in small mammals and humans in the coastal region of Zhejiang Province, China. *J Med Virol* **82**, 987-995

Acknowledgement

This paper embodies the hard work of every team member, without their contribution, this paper could not become such fruitful. Here I sincerely thanks to everybody joined this project and helped me a lot.

Firstly, I appreciate my research supervisors, Professor Hiroaki Kariwa, Laboratory of Public Health, Faculty of Veterinary Medicine, Hokkaido University; Professor Ayato Takada, Division of Global Epidemiology, and Lecturer Keita Matsuno, Division of Risk Analysis and Management, both in the International Institute for Zoonosis Control, Hokkaido University. Their guidance and constructive advice helped me to decide the direction of my study, made conclusions from the data and improve the quality of this thesis.

Also, I must thank my supervisor, Kumiko Yoshimatsu, an associate professor at the Institute for Genetic Medicine. I have learnt a lot of experiment techniques and basic knowledge from her, and she gave me plenty of thoughtful suggestions and advice when I discussed with her about my new ideas. She showed me a path to find out how to figure out the problem, how to design an experiment to solve the problem, and finally how to learn from the whole process. As my supervisor, she was not only concerned on teach me the necessary knowledge, but also helped me tremendously in my growth as an independent researcher. On the other hand, as a foreigner student, she is also my Japanese teacher and provided me a good environment to practice my Japanese, when I made mistakes, she corrected me with patient instead of laughing or blaming, this courage me a lot to speak Japanese more bravely. Following her leading, I can feel my growth as a person.

Also, I will never forget the help from the Professor Jiro Arikawa and associate professor Yoshimi Tsuda from Nagasaki University, and Lecturer Kenta Shimizu from Gunma University. As the initial members of Arikawa's laboratory, Arikawa sensei gave me a chance to start my PhD in this lab to learn the animal experiment techniques

and taught me how to enjoy the lifestyle as a researcher, this helped a lot when I was trying to get through the obstacles and hard times. Tsuda sensei showed me a standard as a wise researcher with broad vision, fast reaction and most importantly, the hard-working attitude. Shimizu sensei was like my elder brother, I can discuss with him about my experiment to learn more acknowledgement, also I can learn some Japanese manner and daily life things from him.

This work would not success without my lab mate's kindness contribution. Rakiiya S. Sarii used his knowledge as a veterinary to helped me with the IHC analyze; Devinda S. Muthusinghe and Sithumini M.W Lokupathirage helped me to do the investigation, data processing, and more importantly, they are my good friends.

In addition, I would like to acknowledge Junko Nio-Kobayashi of Graduate school of Medicine, Hokkaido University for her direct involvement in the pathological analysis throughout this study.

This study will not be established without the DX doctoral fellowship and WISE program support. The funding gave me a chance to implement my ideas, also provided me a stage to communicate with the researchers from other fields which broad my vision.